ASSESSMENT OF THE EFFECT OF BEAM MODIFIERS ON SKIN DOSE FOR EXTERNAL BEAM RADIOTHERAPY USING GAFCHROMIC EBT2 FILMS

By

Komakech Ignatius

(10435670)

THIS THESIS IS SUBMITTED TO THE DEPARTMENT OF MEDICAL PHYSICS,
SCHOOL OF NUCLEAR AND ALLIED SCIENCES,
UNIVERSITY OF GHANA, LEGON

IN PARTIAL FULFILMENT OF THE REQUIREMENTS FOR THE DEGREE OF

MASTER OF PHILOSOPHY

IN

Medical physics

JULY, 2015

DECLARATION

This thesis is the result of research work undertaken by Komakech Ignatius in the Department of Medical Physics, School of Nuclear and Allied Sciences, University of Ghana. The research was done under the supervision of Prof. A.W. Kwame Kyere, Prof. J. H. Amuasi and Mr. Samuel N. A Tagoe, all from the department mentioned above. It contains no material previously published by another person, nor material which has been accepted for the award of any other degree of the School, except where due acknowledgement has been made in the text.

…… Date ……

Komakech Ignatius

(Student's ID: 10435670)

…… Date ……

Prof. A.W.K. Kyere

(Principal supervisor)

…… Date ……

Prof. J. H. Amuasi

(Co-Supervisor)

…… Date……

Mr. Samuel Nii Adu Tagoe

(Co-Supervisor).

DEDICATION

This thesis work is dedicated to God the Almighty for the great love, care, provisions, encouragements, strength, protections and blessings he has given me throughout my education and above all for the wisdom He has been granting me since secondary school till this MPhil degree.

ACKNOWLEDGEMENTS

I am so grateful to the International Atomic Energy Agency for making it possible for me to undertake this Master of Philosophy Degree programme in Medical Physics in Ghana, and for the continued support they have been providing during the study period.

In a special way, I am particularly grateful to Prof. A.W. K. Kyere, Prof J.H. Amuasi and Mr. S.N.A Tagoe for their continued pieces of advice, corrections, directions, comfort, sacrifices and above all the love and commitments they had in helping me through with my work. No word can express my joy of having you as my team of my supervisors.

Am also grateful to Brother Elio Lucio of St. Mary's hospital Lacor and the government of Uganda for the scholarships they offered me through secondary school and the undergraduate degree programme respectively. This allowed me to have the basic foundation needed for this MPhil course.

Lastly but not the least, am so grateful to Mr. Evans Sasu of KBTH, Mr. George Acqiah of SGMC and the whole MPhil Medical Physics class of 2013-2014 for their willingness to help whenever I needed help.

TABLE OF CONTENTS

LIST OF FIGURES

Figure **Page**

LIST OF TABLES

LIST OF PLATES

LIST OF ABBREVIATIONS

KBTH	Korle Bu teaching Hospital
MPHIL	Masters of Philosophy
SGMC	Sweden Ghana Medical Center
MV	Mega voltage
PMMA	Polymethylmetacrylate
SSD	Source to surface distance
MLC	Multileaf collimator
ICRU	International Commission on Radiation Units and Measurements
MW	Motorized wedge
PW	Physical wedge
ICRP	International commission on radiological protection
CT	Computed tomography
CPE	Charge particle equilibrium
ERS	Electron range surface
OF	Obliquity factor
PDD	Percentage depth dose
TLD	Thermoluminescence dosimeter
EBRT	External Beam Radiotherapy
IMRT	Intensity Modulated Radiotherapy
PP	Parallel plate
RGB	Red green blue

TG	Task group
TBI	Total body irradiation.
2-D	Two dimensional
3-D	Three dimensional
IAEA	International Atomic Energy Agency
TECDOC	Technical documentation
TRS	Technical Reports Series

ABSTRACT

In radiotherapy, a patient may present irregular surface contour at the point of beam entry and this coupled with tissue heterogeneities within the irradiated region would pose problems for dose optimization if beam modifiers are not used. Skin dose is of great concern in external beam radiotherapy with megavoltage beam as the skin is very radiosensitive, and there is the need to minimize radiation dose received by the skin. The use of beam modifiers affects the skin dose and the level of their influence on skin dose needs to be investigated. The purpose of this study was to assess the effect of different beam modifiers on the skin dose for ^{60}Co and 15 MV photon beams. Skin doses were measured for solid water (PMMA) phantoms with Gafchromic films. It was observed that, skin dose for all the beam modifiers as well as that for the open beams increases as field size increases. At SSD of 80 cm, skin doses for 10 x 10 cm^2 and 25 x 25 cm^2 were, 36.9%, and 61.8% respectively for the ^{60}Co unit. It was observed that, for a particular field size, skin dose for the 15 MV photon beam was much lower than that for ^{60}Co beam, which gives an advantage of using the 15 MV photon beam over ^{60}Co beam. As SSD increases skin dose reduces for both ^{60}Co and 15 MV photon beams. For wedged fields (with 60º motorized wedge), it was found that there were very little effects on skin dose for smaller fields but significant effects for the larger fields (≥15 x 15 cm^2) as compared with open beams for the 15 MV photon beam. Skin dose for bolus was higher compared with that of open beam and were 57.4% and 73.8% for 10 x 10 cm^2 and 20 x 20 cm^2 at 100 cm SSD respectively. For ^{60}Co beam, the physical wedges and the 1.5 cm thickness compensator greatly reduced skin doses as compared to all the other beam modifiers. The skin doses for 10 × 10 cm^2 field were 21.3%, 19.4%, 18.7%, 19.1% and 23.6% for 15º, 30º, 45º, 60º and the 1.5 cm thickness compensators respectively,

at SSD of 80 cm). These compared with 35.4% and 33.7% for the tray and open fields at the same SSD and field size as those for the wedges and compensator above. Skin doses reduced as the compensator thickness was increased.

CHAPTER ONE

INTRODUCTION

1.1 Background

After the discovery of the x-rays by Roentgen in 1895, and radioactivity phenomenon in 1896 by Henry Becquerel, the use of ionizing radiation as a means of cancer treatment was soon appreciated. Since then, radiation therapy has improved and developed into an important specialized medical field. Radiotherapy is used in the treatment of disease, primarily malignant tumours, using electromagnetic and particle radiations. The patient can be treated with external beam (teletherapy), or by radiation source placed in close proximity to the target (brachytherapy).

The treatment prescribed can either be for curative or palliative intention. In the case of curative purposes, the side effects are sometimes unavoidable, but they are accepted as an inevitable part of the cure. On the other hand, palliative radiotherapy is given to patients with advanced cancer cases when the cancer is already spread and this type of treatment would not cure it. The aim of this type is to slow down the growth of the malignant tumour and reduce symptoms such as pain.

External beam radiation therapy uses medical linac and ^{60}Co units for cancer treatment and the methods of treatment used depend on different factors such as;

i. shape and site of the target or tumor to be treated within the patient

ii. sparing of normal tissues within the vicinity of the target from excessive irradiation

iii. financial constraints and the quest of optimization of radiation dose to the target.

Skin dose should be negligible during this treatment delivery, but this is never achieved because it depends on secondary electrons [**1**] . These secondary electrons are produced by the interactions of photons with scattering materials such as the collimator jaws, air, patient's skin, beam modifiers etc. Nilsson 1986, [**2**] has shown that the air column under block tray has a more significant contribution at lower energies. Treatment head materials and setup parameters are the sources of contamination electrons which together with low-energy photons affect surface and buildup region dose. So, optimization of a treatment plan requires appropriate beam directions, number of fields, beam weights, and intensity modifiers (e.g., wedges, compensators, multileaf collimators (MLC), bolus etc.).

These beam modifiers however also affect the skin dose for a particular treatment delivery where they may be used, by affecting the scattering of electrons.

Therefore, accurate assessments of surface and superficial doses in radiotherapy can provide valuable information for clinical consideration while at the same time limiting severe skin toxicity, especially for breast, pelvis and head-and-neck treatments as dose at the skin is primarily due to electron contamination from the flattening filter and beam modifiers.

The aim of this study was therefore to assess the skin doses for different beam modifying devices at various source-to-surface distances (SSDs) used at Korle-Bu Teaching Hospital and Sweden Ghana Medical Centre (SGMC).

1.2 Problem statement

In radiation therapy, there is a high possibility of encountering irregular patient's surfaces at the point of beam entry. This, coupled with tissue heterogeneities, affects dose

distribution at depths. These irregularities need to be corrected using the beam modifiers, so that a uniform dose distribution within +7% and -5% *(ICRU report 50, 1993* [**3**]) of the dose prescription can be achieved. This way, we avoid exceeding the tolerance dose of the critical structures around tumor volume.

However when beam modifiers are used, the dose delivered to the skin during treatment is changed and in some cases a high dose is deposited at the skin leading to the destruction of the skin sparing effect as was reported by Daniel in April 1896 [**4**] as well as Becquerel in 1901 who also reported reddening of the skin after prolonged radiation exposure [**4**].

Therefore, it is important to understand how each of these beam modifiers affect skin dose before treatment because of the possible biological complications. Moreover, in radiotherapy each treatment unit is unique and requires its own specific parameters such as beam data for accurate treatment delivery. Therefore the available information does not completely apply to every treatment machine but rather a guide for an accurate one.

1.3 Objectives

The main objective of this study was to assess the effects of selected commonly used beam modifiers on skin doses for patients undergoing cancer treatment using external beam radiation therapy at the oncology department of Korle-Bu Teaching Hospital (KBTH) and Sweden Ghana Medical Centre (SGMC).

The specific objectives are:

- to measure and evaluate the skin doses for different beam modifiers under different fields, SSDs, energy and their corresponding doses for open fields.
- to determine the percentage skin dose in relation to d_{max} dose for these different beam

modifiers used.

- to compare the percentage skin doses that result from the Equinox 100 ^{60}Co unit at Korle-Bu National Centre for Radiotherapy and Nuclear Medicine and from the Synergy 11 linear accelerator at SGMC.

1.4 Relevance and justification

In radiotherapy, cancer patients with head and neck, prostate, lung, esophageal, breast cancers present with irregular surfaces and tissue heterogeneities [**5**]. It is evident that unmodified fields give rise to unacceptable dose distributions within the target volume and excessive irradiation of sensitive structures. Therefore optimization of a treatment plan requires appropriate beam directions, number of fields, beam weights, and intensity modifiers (e.g., wedges, compensators, bolus, trays, multileaf collimators (MLC), etc.). These help to generate uniform dose distributions to the tumours and allow the sparing of normal healthy tissues. However, these beam modifiers also affect skin doses whenever they are used. Therefore understanding how each affects skin dose in a particular treatment unit is of great importance. This will ensure that medical physicists take into account their effects and hence make appropriate setup and other adjustments to keep the appropriate dose to the skin.

1.5 Scope and limitation

The scope of this thesis is in the area of radiotherapy, and particularly in skin dose that results from the use of beam modifying devices to produce desired intensities and shielding of organs. These beam modifiers include: physical wedges (PW), cerrobend

compensators, bolus, motorized wedge (MW) and acrylic block tray. Measurements were taken with Equinox 100 ^{60}Co treatment unit at Korle-Bu National Centre for Radiotherapy and Nuclear Medicine and with a Synergy 11 linear accelerator treatment unit at Sweden Ghana Medical Centre using GafChromic EBT2 films.

1.6 Organization of thesis

This thesis is in a chronological order of five chapters. Chapter one is an introduction to the research and provides an overview of the current state of knowledge relevant to the study. Chapter two reviews existing literature relevant to the research problem. Chapter three focuses on the experimental and theoretical framework for the study. The results obtained are presented and discussed in chapter four. Chapter five contains the conclusions of the study, recommendations and suggestions for further research.

CHAPTER TWO

LITERATURE REVIEW

2.1 Introduction

During external beam radiotherapy, the skin is at risk from radiation effects such as erythema, skin peeling and necrosis. Epidemiological studies have also found an association between radiotherapy and basal cell carcinoma [**6**]. However, skin dose is complicated because of the different skin layers with various depths of thickness that varies between patients and locations on a given patient. The ICRP [**7, 8**] recommends assessing the skin dose at depth of 0.07 mm for the basal layer which is taken as the surface dose, while dermal layer may be assessed at 1.0 mm. Although treatment planning system can calculate skin dose generally within ± 25% accuracy, this however requires CT images as well as a calculated treatment plan [**2**]. A method to measure skin dose on the central axis as a function of treatment parameters was proposed by Lamb and Blake [**9**]

2.2 Skin and buildup region doses

In external beam radiotherapy, patients treated with megavoltage beams have lower surface skin dose compared with the maximum dose that occurs in deeper tissues. In contrast, lower energy beams give rise to maximum ionization at or close to the skin surface [**10**]. Initial electronic buildup of MV beams increases with depth which results in a reduced surface dose and maximum dose at the equilibrium depth. The dose region between the surface, depth = 0.0 cm and depth d = d_{max} in megavoltage photon beams is the buildup region and results from relatively long range of energetic charged particles (β^-

and β^+) that are first released in the patient by photon interactions and finally deposit their kinetic energies in the patient. Immediately beneath the patient's skin surface, the condition of charge particle equilibrium (CPE) doesn't exist and the absorbed dose is then much smaller than collisional kerma. However, as the depth in the patient increases, CPE is eventually reached at d = d_{max} where d is approximately equal to the range of the secondary charged particles and the dose becomes comparable with the collisional kerma. Beyond d = d_{max}, both collisional kerma and absorbed dose decreases due to the attenuation of photons in the patient that results in transient rather than true CPE [**11**].

This lower surface dose as compared with the maximum dose is referred to as skin sparing and represents an important advantage of megavoltage beam over orthovoltage and superficial beams in the treatment of deep seated lesions. Orthovoltage and superficial beams do not exhibit skin sparing since the maximum dose occurs at the skin surface (i.e. the surface dose equals the maximum dose). Skin sparing is one of the most desirable qualities of high-energy photon beams. However, this feature can be reduced if there is excessive electron contamination [**11**].

2.2.1 Electron contamination of photon beams

Skin dose arises from electron contamination of the incident radiation beam as well as the backscattered photons and electrons from the scattering medium. All x-ray and γ-ray beams used in cancer treatment are known to be contaminated with secondary electrons. These electrons come from photon interactions that occur in the collimator, air, and in any other material in the path of the beam that scatters photons. The use of shadow tray to

support beam-shaping blocks and the column of air between the skin surface and tray produces secondary electrons which can significantly increase skin dose. [**10**].

In the build-up region, depth dose increases with increasing field size leading to a shift in d_{max} to increasingly shallower depths [**10, 12**]. This cause of d_{max} shift with field size has been studied by several researchers and the current evidence shows that this effect is predominantly caused by secondary electrons [**7, 13, 14**].

2.2.2 Skin sparing as a function of photon energy

Studies indicate that dose distribution on the skin depends on many variables such as field size, beam energy, SSD, and configuration of secondary blocking tray [**10, 12, 15**]. While some studies have found a reduction in skin dose at higher megavoltage energies [**6, 16, 19**], other studies have not, in particularly for larger field sizes as demonstrated with lower energies (6-10 MV) and higher energies (15-18 MV). ^{60}Co on the other hand produces a higher surface dose that also increases with field size, and ranged between 20% - 85% of d_{max} dose [**6**] for open beam. Table 2.1 is an example, but is not universal for all treatment machines especially for depths less than 2 mm, however reasonable agreement between different treatment machines has been shown to exist for greater depths [**10**].

Table 2. 1: Build-up dose distribution in polystyrene for a 10 x 10 cm^2 field.

depth (mm)	^{60}Co 80 cm	4 MV 80 cm	10 MV 100 cm	25 MV 100 cm
0	18.0	14.0	12.0	17.0
1	70.5	57.0	30.0	28.0
2	90.0	74.0	46.0	39.5
3	98.0	84.0	55.0	47.0
4	100.0	90.0	63.0	54.5
5	100.0	94.0	72.0	60.5
6	-	96.5	76.0	66.0
8	-	99.5	84.0	73.0
10	-	100.0	91.0	79.0
15	-	-	97.0	88.0
20	-	-	98.0	95.0
25	-	-	100.0	99.0
30	-	-	-	100.0

Data from the Physics of Radiation Therapy, Khan 2003 [**10**].

As can be seen from table 2.1, a tissue equivalent bolus of 5 mm of thickness is adequate for ^{60}Co beam to achieve 100% buildup of dose. In general, more and more pronounced skin sparing can be achieved with high energy beams, not only for the skin surface but also for the subcutaneous tissues. It has been also noted in [**11**], that the higher the photon beam energy, the lower the surface dose, which for a 10 x 10 cm^2 field typically amounts to 30% of the d_{max} dose for a ^{60}Co ɤ-ray beam, 15% for a 6MV x-ray beam and 10% for an 18 MV x-ray. Buston et al. 1998 [**17**] also measured skin doses on the central axis of the beam relative to d_{max} for a 10 x 10 cm^2 field size and found them to be 22%, 17% and 15.5% for 6 MV, 10 MV and 18 MV photon beams respectively.

2.2.3 Effect of absorber-skin distance

With no absorber placed in the beam, electron contamination is mainly caused by the secondary electron emission from the collimator (including source, flattening filter, and air). But when an absorber of thickness greater than the range of secondary electrons

(equilibrium thickness) is introduced in the beam, the collimator electrons may almost be completely absorbed but the absorber itself becomes the principal source of electron contamination of the incident beam. By increasing the distance between the tray and the skin surface, the electron fluence incident on the skin is reduced due to the divergence as well as absorption and scattering of electrons in air. Therefore, skin sparing is enhanced by placing the shadow tray farther away from the skin surface. In the case of a ^{60}Co γ-ray beam, it has been found [**10, 18**] that for small field sizes, an air gap of about 15 to 20 cm between the scatterer and the skin surface is adequate to keep the skin dose to an acceptable level (< 50% of the d_{max},). This has been found to be true for higher-energy beams as well [**14**]. Figure 2.1 shows the effect a lucite shadow tray placed in the beam at various distances from the phantom surface on the dose distribution in the build-up. Not only does the relative surface dose increase with decreasing tray-to-skin surface-distance but the point of maximum dose buildup moves closer to the skin surface. Figure 2.1 also illustrates the principle of what is known as the "beam spoiler", where a low atomic number absorber such as a lucite shadow tray when placed at an appropriate distance from the surface can be used to modify the build-up curve.

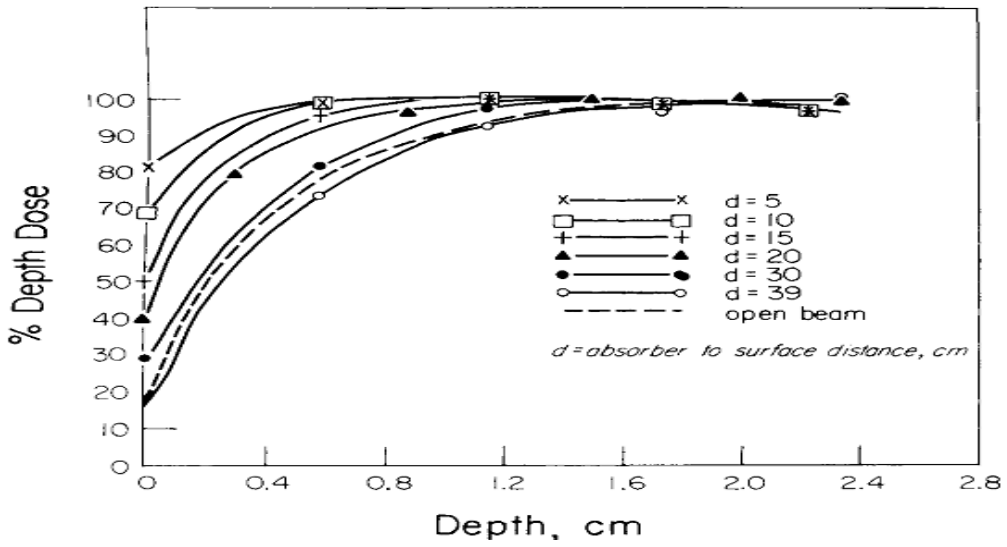

Figure 2. 1: Effect of lucite shadow tray on dose buildup for 10-MV x-rays. Percent depth dose distribution is plotted for various tray-to-surface distances (d). 10-MV x-rays, tray thickness = 1.5 g/cm2, field size = 15 x 15 cm, SSD = 100 cm, and SDD = 50 cm. [**10**].

2.2.4 Effect of field size on skin/surface dose

Yadav et al. 2009 [**1**], carried out skin dose estimations for various beam modifiers at various SSDs for 6 MV photon where surface and buildup region doses were measured using an acrylic slab phantom and a Markus parallel plate ionization chamber. They carried out measurements for open fields, motorized wedge fields, and for acrylic block tray fields ranging from 3 x 3 cm^2 to 30 x 30 cm^2. In their work, they showed that as the field size increases, so does the skin dose for all the beam modifiers. For the block tray, they concluded that electrons were eliminated from the upstream but generated its own new secondary electrons. The number of electrons produced upstream were more than the ones eliminated downstream by the tray, and therefore skin dose increased. For the 60^o motorized wedge fields, they found out that the skin dose increased as the field size was increased but were lower than for open fields. Physical wedge both eliminated electrons

from upstream and generated electrons by itself; with the number generated being less than the ones eliminated for smaller field size [**1, 6**].

This increase in skin dose with field size generally, is as a result of increased electron emission from the collimator and air [**10**]. Figure 2.2 is a plot of relative surface dose as a function of field size for ^{60}Co, 4 MV and 10MV photons. These data show that skin sparing is significantly reduced for the larger field sizes.

Saylor and Quillin [**19**] have discussed the relative importance of field size and tray-to-skin surface distance for ^{60}Co gamma rays. They have shown that the optimum skin sparing occurs for the ratio of $\frac{h}{r}$ of about 4, where *h* is the tray-to-skin surface distance and *r* is the radius of an equivalent circular field. This ratio can be easily achieved for smaller fields like *5* x *5* cm, because it requires a distance of 12 cm while for the 30 x 30 cm field, the corresponding absorber-surface distance is 67 cm, which is impossible for isocentric treatments. It is therefore necessary to use electron filters when using large fields with a tray-to-skin distance of 15 to 20 cm.

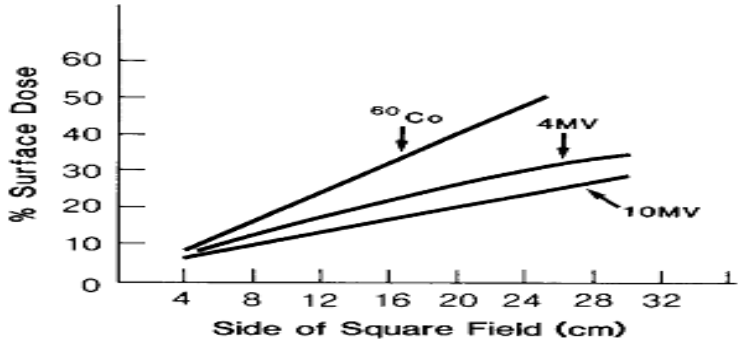

Figure 2. 2: Percent surface dose as a function of field size. ^{60}Co, Theratron 80, SSD = 80 cm, SDD = 59 cm. 4 MV, Clinac 4, SSD = 80 cm. 10 MV, LMR 13, SSD = 100 cm, SDD = 50 cm. ^{60}Co and 4-MV. (Data are from Khan, 2003 [**10**]).

2.2.5 Effect of electron filters on skin/surface dose

Skin dose can be reduced by using γ-ray absorbers of medium atomic number (Z in the range of 30-80) commonly known as electron filters. Their introduction in the photon beam reduces the secondary electron scatter in the forward direction. Hine [**20**] studied the scattering of electrons produced by γ-rays in materials of various atomic numbers and showed that the medium atomic number absorbers give less electron scatter in the forward direction than either the low or the very high atomic number materials.

Khan (**21**) and Saylor and Quillin (**19**) applied the results of Hine's study to the design of electron filters for the purpose of improving skin dose for $^{60}C_o$ teletherapy. It was later shown that such filters not only reduce the surface dose but also improve on the build-up characteristics of large fields [**7**]. Figure 2.3 is a plot of relative surface dose as a function of log (Z+ 1).These data are plotted in this manner to show agreement with the theoretical relationship discussed by Hine [**20**].

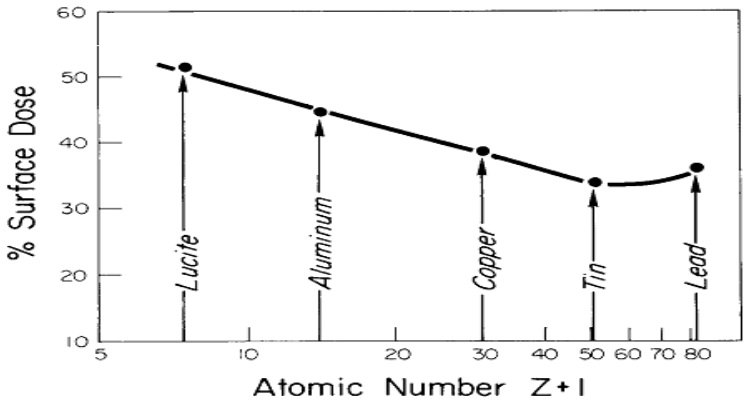

Figure 2. 3: Variation of percent surface dose with atomic number of absorber, with each having thickness of 1.5 g/cm^2 and was mounted underneath a lucite shadow tray. 10-MV x-rays, field size = 15 x 15 cm and absorber-to-surface distance = 15 cm. (Data from Khan [**10**])

As the atomic number *Z* increases, the surface dose falls to a shallow minimum (Z = 50 is for tin) due to increased electron scattering in the absorbers. Further increases in *Z* result in increased surface dose due to increased production of photoelectrons and electron pairs in addition to the Compton electrons. These results qualitatively agree with those obtained for ^{60}Co γ-rays [**19, 20**]. Saylor and Quillin [**19** have suggested the use of leaded glass as an electron filter so as to preserve the light field.

2.2.6 Skin sparing at oblique incidence

It has been shown that skin dose increases with increasing angle of incidence [**22, 23**], though there is little dosimetric impact for smaller angles (<40°) but with greater increase for larger angles (e.g. 50% at 55°) [**6**].

Clinically, brisk reactions have been reported in patients when the beam is incident nearly at glancing angles. Jackson [**24**] used the concept of electron range surface (ERS) which is a 3D representation of the secondary electron range and distribution produced by a pencil beam of photons interacting with the medium to explain the increase in skin dose with increasing angle of incidence. Electrons generated inside the ERS volume will reach point, P, (Fig. 2.4) and contribute to the dose there, while those generated outside make no contribution because of their inadequate range. For ^{60}Co γ-rays, it's reported that the ERS is in the shape of an ellipsoid with axial dimensions of 5 x 2.4 mm [**24**]. Due to the electron contribution from the portion of the ERS, which appears below the phantom surface (hatched curve), an increase in the angle of incidence of the photon beam results in additional surface dose at point, P, (Figure 2.4). Tangential beam incidence with half

of the ERS below the phantom surface have an upper estimate of the dose to the skin given by the relationship [**23, 24**]:

$$\text{Percent skin dose} = \frac{1}{2}(100\% + \text{entrance dose}) \quad \ldots\ldots\ldots\ldots\ldots\ldots\ldots\ldots\ldots\ldots \quad 2.1$$

where the entrance dose is the surface dose for normal incidence expressed as a percentage of d_{max}.

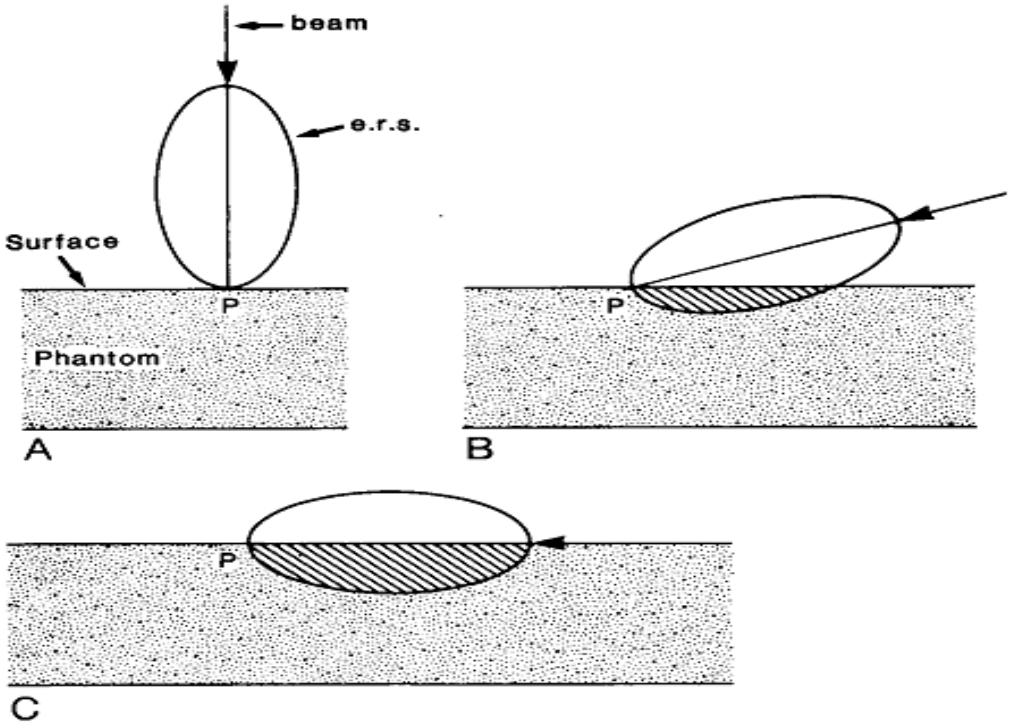

Figure 2. 4. The use of ERS to determine surface dose buildup at point P. A: Perpendicular beam incidence. B: Oblique beam incidence. C: Tangential beam incidence [**10**].

Skin doses for other incidence angles lie between the values for the normal and the tangential incidence. Gerbi et al. [**15**] carried out a systematic study of dose buildup for obliquely incident beams as a function of depth, field size, energy (6-24 MV), angle, and

SSD. A quantity called *obliquity factor* (OF) was defined as the dose at a point in phantom on central axis of a beam incident at angle **θ⁰,** with respect to the perpendicular to the surface, divided by the dose at the same point and depth along central axis with the beam incident at an angle of **0⁰ [10, 25, 26**]. This obliquity factor represents dose enhancement due to beam obliquity for the same depth. It is observed that, the depth of maximum dose buildup decreases as the surface dose increases with the incidence angle. Maximum dose value is reached faster at glancing angles than at perpendicular incidence and as a result of this, the dose build-up region is compressed into a more surface region. Under this condition, a high skin reaction becomes much more likely **[25].**

2.2.7 Effects of SSD and setup on surface dose

Experimental results show that skin dose increases slightly as SSD decreases, though the effect is relatively small (≈ 10% for SSD varying between 85 cm – 100 cm or 100 cm-120 cm), but for larger fields (≥ 20 x 20 cm^2) it can exceed 20 % when other modifying devices such as block is used. Yadav et al, 2009 [**1**] measured skin dose for small fields (10 x 10 cm^2) at SSDs of 80 cm, 100 cm and 120 cm and the values were 15.5%, 14.5% and 15.5% respectively. Maximum percentage skin dose deviation measured by Batson. M.J. [**27, 30**] was 4.0% for SSD from 80-120 cm.

2.3 Exit dose

In external beam radiotherapy, substantial skin dose comes from the beams exiting the patient with megavoltage treatment units. However, due to the lack of back scatter material beyond the patient's exit surface, the skin dose is less than predicted by PDD by about 15% (relative difference) [**6**]. Although full scatter conditions are achieved (as predicted by PDD) with minimal material, including virtually any immobilization device behind the patient [**6, 28**].

2.4 Plastic phantom

Plastic phantoms are used for ionmetric measurements in the buildup region, and normally are made of polystyrene or water equivalent plastic phantoms. A useful configuration for these phantoms consists of several blocks measuring 30 x 30 cm^2 but of different thicknesses. One block (2 cm thickness) has a hole drilled in it such that the center of the hole is 1 cm from one surface to accommodate a Farmer type ionization chamber. One block is machined to place the entrance window of a parallel plate ionization chamber at the level of one surface of the block.

This arrangement allows measurements with no material in the radiation beam. Additional blocks of same material as the rest of the phantom should be 30 x 30 but with thicknesses of 0.5, 1, 2, 4, 8, 16 and 32 mm. These, combined with the 5 cm blocks, allow measurements of depth dose in 0.5 mm increments to any depth from the surface to 40 cm with the plane ionization chamber and Farmer type chamber [**11**].

2.5 Radiation dosimeters for skin dose measurements

A radiation dosimeter is an instrument, device or a system that can measure or evaluate, either indirectly or directly, the quantities: exposure, kerma, absorbed dose or equivalent dose, or its time derivatives (rates), or related quantities of ionizing radiation. It is capable of providing a reading that is a measure of the average absorbed dose deposited in its (the dosimeter's) sensitive volume by ionizing radiation. A dosimeter along with its reader is referred to as a dosimetry system. To function as a radiation dosimeter, the dosimeter must possess at least one physical property that is a function of the measured dosimetric quantity and that can be used for radiation dosimetry with proper calibration.

However, due to the steep dose gradient in the buildup region, the size of the radiation dosimeter should be as small as possible along the incident beam. Due to this condition, extrapolation chambers are the instruments of choice for the measurements [**10**]. However, only a few centers have these instruments available and instead, the fixed-separation plane parallel ionization chambers are commonly used for this purpose. In addition to ionization chambers, thin layers (< 0.5 mm) of TLD material [**29**] and radiochromic films such as GafChromic films are available for the measurements of skin dose. The film is first calibrated within the dose range required before use [**10, 30**]. For this work, the choice of gafchromic films mas made due to its availability.

2.5.1 Ionization chambers

Ionization chambers are radiation dosimeters used in radiotherapy and diagnostic radiology for determination of radiation dose. It is basically a gas filled cavity that is surrounded by a conducting outer wall and collecting electrodes which are kept apart with

a high quality insulator so as to reduce the leakage current when a polarizing voltage is applied to the chamber. Further chamber leakage is reduced by using a guard electrode that intercepts the leakage current and allows it to flow to the ground, bypassing the collecting electrode. Better charge collection due to improved field uniformity in the sensitive/active volume of the chamber is another advantage. However, temperature and pressure corrections are required when taking measurements with open air ionization chambers. These corrections accounts for the change in the air mass in the chamber volume as a result of change in ambient temperature and pressure. Particularly, for skin dose measurements are the fixed plate ionization chambers and the extrapolation chambers [**10, 31, 32**].

2.6 Electrometers

These are devices for measuring small currents (~10^{-9} Å or less). They are high gain, negative feedback operational amplifier with a standard resistor or a standard capacitor in the feedback path to measure the ion chamber current or charge collected over a fixed time period.

2.7 Radiochromic film

There are several methods that have been used to measure skin doses. For this work, the method chosen involves using radiochromic films e.g. GafChromic film (e.g. HD-810 film, DM-1260, EBT, EBT2, EBT3, MD-55 and MD-55-2 film with effective depth of skin dose measurement at 0.17mm ± 0.03mm). They are colourless films with nearly

tissue equivalent composition (9.0% hydrogen, 60.6% carbon, 11.2% nitrogen and 19.2% oxygen) that can change colour from light to dark blue colour upon exposure to radiation. They contain a monomer crystal in a gel bound to a mylar (polyethylene terephthalate) substrate, a special dye that gets polarized when exposed to radiation. When this polymer absorbs light, the transmission of light through it can be measured with a suitable densitometer or a scanner. The film's response to radiation exposures less than 50 mGy is not noticeable and the flatbed scanner cannot pick up the small changes in film color [**34**].

Radiochromic film is a relative dosimeter but with proper care taken during calibration and the environmental conditions, a precision better than 3% can be archived [**10**].

Other roles played by the film include checking the alignment of the size and shape of radiation fields, leakage radiation around collimators and positioning of special radiation fields [**33**].

2.7.1 Introduction

GafChromic EBT2 film used in this work is a radiochromic film that has been specifically developed to address the need of a medical physicist working in radiotherapy environment. It is used in quantitative measurement applications in external beam radiotherapy (EBRT), in particularly in IMRT, skin dose and brachytherapy. In common with the other previous versions above, GafChromic EBT2 film is self-developing, but it also incorporates numerous improvements in ISP's (International Specialty Product) radiochromic film technology. Some of the features include;

a) measure with an economic flatbed colour scanner.

b) dose range 1 cGy – 10 Gy (measure in red colour channel); up to 40 Gy measured in green colour channel.

c) uniformity is better than ±3% in dose.

d) density changes stabilize rapidly after exposure.

e) Stable at temperatures up to 60^{o}C.

f) energy – dependence :< 10% response difference from 60keV into the MV range.

g) handle in room light- eliminate the need for a dark room.

h) water resistant and can be immersed in water phantom for hours.

i) has high spatial resolution- can resolve features to at least 100µm.

2.7.2 Configuration and structure of GafChromic EBT2

GafChromic EBT2 is made by laminating an active layer between two coatings. The EBT2 laminate is identified by its batch number. The film is comprised of a single active layer, normally 30µm thick, containing an active component, a marker dye stabilizer and other components giving the film its energy-independence response. The configuration of GafChromic EBT2 is shown in Figure 2.5 below.

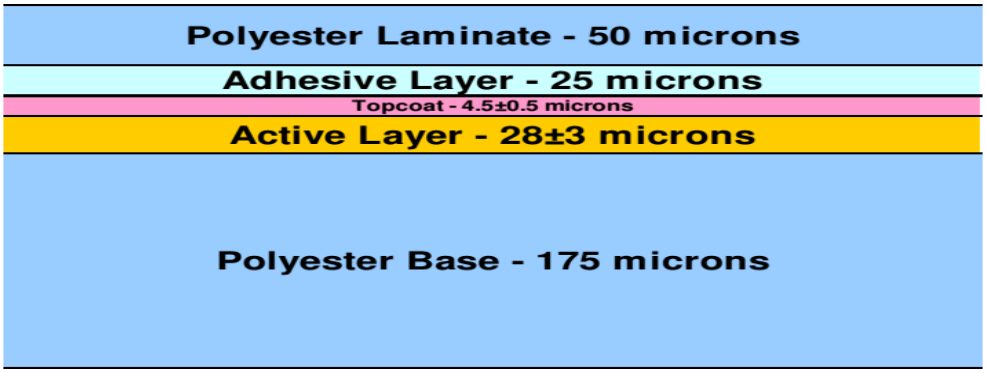

Figure 2. 5: Configuration of GafChromic EBT2 dosimetry Film. (Data from [**34**])

2.7.3 GafChromic EBT2 Dosimetry film characteristics

This high sensitivity radiochromic film has been designed for the measurement of absorbed dose of high-energy photons used in IMRT. The film has been designed to measure doses up to at least 30 Gy when used with an RGB color scanner. At doses above 10 Gy the response in the red color channel approaches saturation, so in the case of single channel dosimetry it is preferable to change to the green color channel for these measurements. EBT2 film has been designed to have a photon response that is nearly energy independent from about 100 keV into the MV range. This is accomplished by the careful design of the atomic composition of the film. For EBT2 lots manufactured after May 2009, the ISP believed that the response of the film to 100 keV and 6 MV photons is within about 5% [3**4, 35**].

2.7.4 Measurement.

GafChromic® EBT2 dosimetry film can be measured with a variety of instrumentation including transmission densitometers, film scanners and spectrophotometers, but the preferred device is an RGB colour scanner. When the active component in the film is exposed to radiation, it reacts to form a blue colored polymer with absorption maxima at about 636 nm and 585 nm. Since the peak absorption in the exposed film occurs at about 636 nm, with a secondary peak at about 585 nm as shown in Figure 2.6; below, the greatest response occurs when measurements are made with red light [**34**].

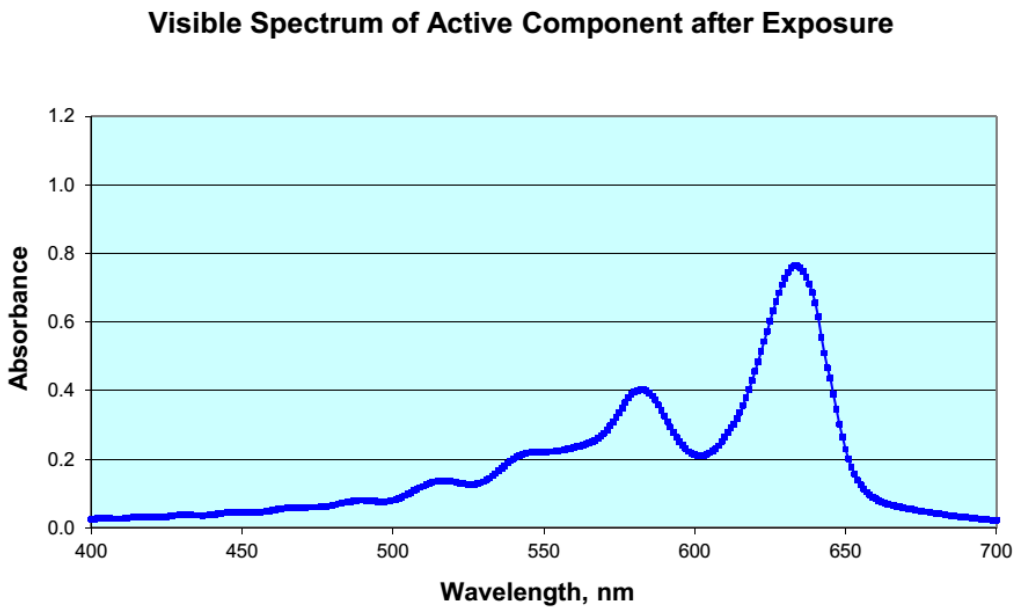

Figure 2. 6. Absorption Spectra of the Active Component in EBT2 Film after Irradiation [**34**].

2.7.5 Film calibration and sensitivity

A calibration of the film's response is the first requirement of a film dosimetry protocol. It is of utmost importance in establishing the accuracy and repeatability of the overall dosimetry measurements and evaluation. The first issue is the size of the calibration films. In an attempt to capture the average film-scanner response, a measuring area of 25 cm^2 is require [**34, 35**].

Calibration of radiochromic film is done using known doses from a large well-characterized uniform radiation field with the film placed on the central portion of a large photon beam (such as; a 40 x 40 cm^2) at depth of interest (preferably $\geq$ 5 cm). The characteristics of the calibration beam should be determined by some other dosimeter (such as an ionization chamber). This would allow direct film calibration in terms of

absolute dose within the dose range of interest. The relationship between absorbed dose and film response should be determined and can then be plotted as a curve, often known as a calibration curve. The slope of the calibration curve decreases as dose increases as indicated in Fig. 2.7 (a). The calibration curve can provide information for conversion of film response to dose and vice versa. The relationship between dose and film response can also be tabulated. The change in film response per unit absorbed dose can be represented by a single number for a net optical density up to 1.0. This number defined as film average sensitivity, is the average change in response (i.e., readout) per unit absorbed dose calculated over the lower, most linear portion of the calibration curve. This number depends on one or more of the following [**33**]: (i) the wavelength used for readout, (ii) the particular densitometer used for readout, (iii) film batch, (iv) the delay between irradiation and readout, (v) beam quality of the calibration source, and (vi) Other factors (such as temperature and humidity).

Figure 2.7 is a plot of (a) net OD and (b) net OD per unit absorbed dose measured two days post irradiation. Figure 2.7 (a) has two fairly linear portions, one from 0 to 30 Gy, and the other one from 30 to 100 Gy. The average sensitivity for the dose range 30-100 Gy drops about 15% as compared to the one for the dose range 0-30 Gy. This average sensitivity can then be used for conversion of film response to dose for these conditions and is clearly inappropriate for higher doses or other conditions [**33**].

Sometimes a calibration function is obtained by exposing a number of steps or patches on a single sheet of EBT2 film. This is very good as long as the area of the film is at least 25 cm^2 and does not include the edges of the film.

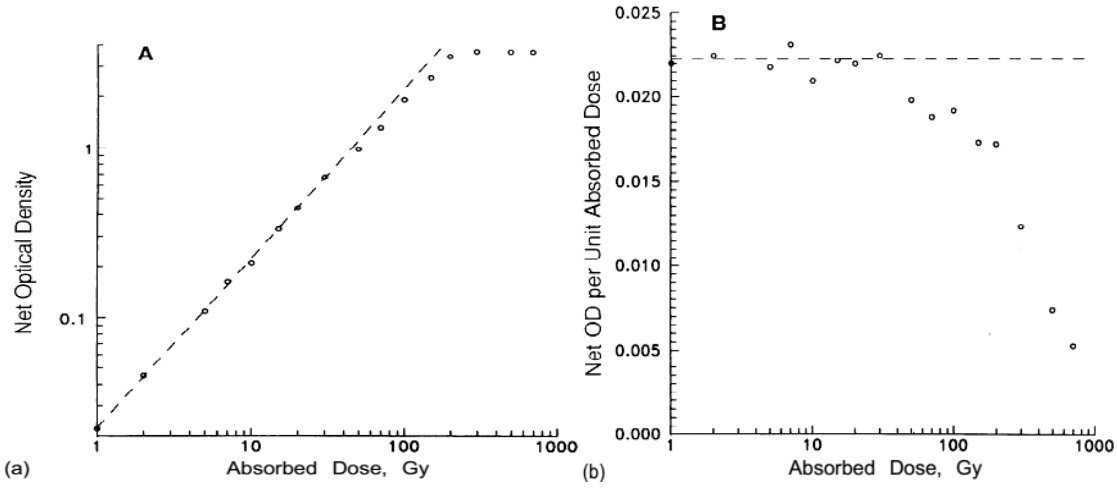

Figure 2. 7: Log plot of (a) net optical density and (b) net optical density per unit dose as a function of dose for MD-55-2 film [**33**].

At high doses, the response values would asymptote to constant as the film gets progressively darker.

Film response = $\frac{(a+b.D)}{(D+c)}$ Where D = dose, a, b and c constants.

2.7.6 Medical applications

The use of radiochromic film in medical applications is extensive ranging from high-dose gamma ray exposures as in brachytherapy to low-dose clinical assessment in vivo such as conventional radiotherapy of breast cancer patients. Below are three medical applications of a radiochromic film [**36, 37**].

(i) Proton dosimetry

Radiochromic films have an elemental composition closer to that of water, which reduces their sensitivity to photon energy for application dealing with determination of dose delivered to water as is given in TG55 **[33]**.

(ii) Skin and surface dosimetry

Due to the low energy dependence, relatively small effective thickness and the ability to produce a two-dimensional dose map which is not currently available in other skin dosimeters in radiotherapy, radiochromic film is a detector for choice. These applications include in-vivo dosimetry as well as phantom studies for dose assessment at the surface, basal and dermal cell layers as well as subcutaneous layers **[33]**.

(iii) Brachytherapy

According to the inverse square law, radiation doses at points close to the source can be very high, which becomes a problem with conventional detectors. Radiochromic film with its low sensitivity and high spatial resolution, has an advantage over other detectors and can be used for dosimetry near these high activity sources **[33]**.

2.7.7 Advantages of GafChromic films.

The following are the advantages of using GafChromic films for dosimetry.

a) Gives permanent absolute values of absorbed dose with an acceptable accuracy and precision.
b) The film has a high spatial resolution.
c) It's easy to handle and analyse.
d) It provides a larger area for dosimetry; including beam profiles.
e) It does not require chemical processing.

Other roles played by the film include checking the alignment of the size and shape of radiation fields, leakage radiation around collimators and positioning of special radiation fields [**33**].

Besides the use of radiochromic films and parallel plate ionization chambers in measuring skin doses, one can use calibrated thermoluminescence dosimetry systems (TLDs). This method has been used for measuring skin doses by many scholars and is reliable. Further information on TLDs and its use in measuring skin doses are given in the literatures [**29, 38**].

2.8 Beam modifiers

2.8.1 Introduction

These are devices that are used to modify the isodose distribution during treatment delivery so that a desirable dose distribution can be obtained or a critical structure can be spared. Treatment planning software for photon beams and electron beams are capable of handling the many diverse beam modifying devices found on linac and ^{60}Co models. Some of these devices are general to all linacs and cobalt-60, whereas others are specific to certain manufacturers. Some of these devices and their specific considerations for incorporation into the TPS are listed in [**11**].

2.8.2 Jaws (Collimators).

Jaws are beam modifiers that help in defining field size by moving independently or in pairs and are usually located as an upper and lower jaws. They may over travel the central

axis of the beam by varying amounts. Asymmetric fields are sometimes used to block off part of a field without changing the position of the isocenter. The independent movable jaws are used to generate rectangular blocking. This is important when matching fields or beam ***splitting*** where the beam is blocked off at the central axis to remove divergence [**10, 11**].

2.8.3 Blocks

Custom designed blocks are still useful in treating small fields (unless mini-MLCs with ultra-small step size are available), mid-field blocking ("island" blocks), or complex field matching [**10**]. Field shielding is accounted for in the TPS by considering the effective attenuation of the block to reduce the total dose under the shielded region. TPSs are able to generate files for blocked fields that can be exported to commercial block cutting machines. The dose through a partially shielded calculation volume, or voxel, is calculated as a partial sum of the attenuation proportional to the region of the voxel shielded. The geometry of straight edge and tapered blocks can be considered separately so as to more accurately model the penumbra through the region of the block edge [**11**].

2.8.4 Bolus.

Bolus is a tissue equivalent (in scattering power and stopping power) material placed directly in contact with an irradiated skin surface to even out the irregular patient contour. Hence, it helps to provide a flat surface for normal beam incidence thereby correcting surface irregularity or give to depth dose distribution a shape appropriate for anatomical

structure to be protected or irradiated. Surface dose is usually increased by placing a layer of uniform thickness bolus (0.5-1.5 cm). However, this does not change the shape of the isodose curves at depth significantly [**39**] and in electron beam therapy, it is used to: (i) flatten out an irregular surface, (ii) reduce the penetration of the electrons in parts of the field, and (iii) increase the surface dose through the provision of buildup dose to the skin surface [**10**]. One of the functions of bolus is preserving the shape of the isodose curves and preventing it from being altered by patient's surface especially where two or more beams are combined to form a resultant distribution [**40**]. However, when use for high energy radiation, has the disadvantage of destroying the skin sparing property since the buildup dose occurs within the bolus itself.

There are a number of commercially available materials that can be used as bolus, e.g., paraffin wax, polystyrene, lucite, superstuff etc. [**11**]. A bag containing a mixture of 60% rice flour and 40% sodium bicarbonate or paraffin wax mixed with approximately equal amount of bee wax is the simplest form of bolus [**41**]. Missing tissues or sloping surfaces are compensated using custom made bolus, built such that one side conforms to the patient's skin and yields a flat normal incidence to the beam. This results in an isodose whose distribution is identical to those produced on a flat phantom; but skin sparing is lost. Bolus is also used to compensate for lack of scatter, such as near the extremities or the head during total body irradiation (TBI).

2.8.5 Tissue compensators

Compensators are beam modifiers normally made from low melting point alloys e.g. cerrobend or lead and are used to produce same effect as the bolus and yet preserve the

skin sparing effect of the megavoltage photon beams. They are custom-made devices that mimic the shape of the bolus but are placed in the radiation beam at least 15 - 20 cm from the skin surface as shown in figure 2.8 below.

When a radiation beam is incident on an irregular or slopping surface of a patient, it produces skewing of the isodose curves and therefore these surface irregularities give rise to an unacceptable non uniform dose distribution within the target volume or causes excessive irradiation of sensitive structures (e.g. the spinal cord). The compensator used to correct this should mimic the effect of the bolus besides preserving the skin-sparing effect.

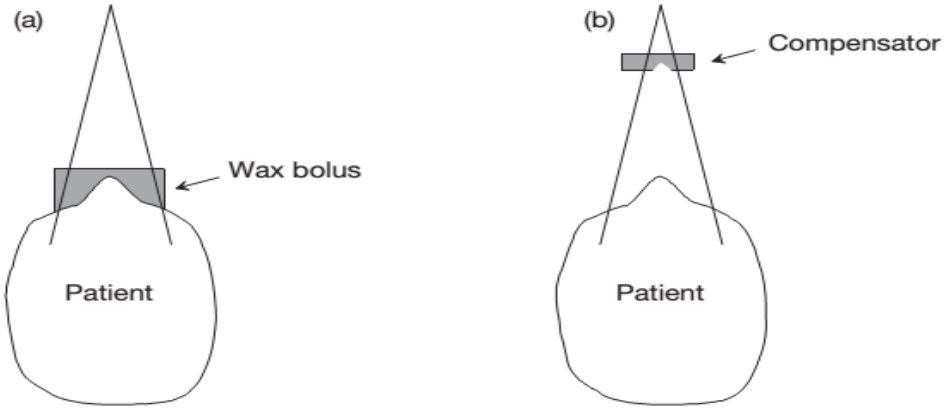

Figure 2. 8: A bolus (a) and a compensator (b) achieving the same dose distribution as in (a) [**11**].

The thickness of the compensator is normally determined on a point by point basis depending on the thickness of the missing tissue. The thickness of compensator *x* along the ray direction above missing tissue can be solved from the attenuation law;

$$\frac{I}{I_o} = exp(-mx) \quad \text{2.2}$$

where, m, is the linear attenuation coefficient for the radiation beam and material used to construct the compensator [**39**]. Further details on tissue compensators including its design can be found in [**40, 42**].

2.8.5.1 Two dimensional (2-D) compensators

In treatment situations where the contour varies significantly in only one direction: along the field width or length, a compensator can be constructed in which the thickness varies only along this dimension. This type of compensator is called a two dimensional compensator.

2.8.5.2 Three dimensional (3-D) compensators

Three dimensional (3-D) compensator systems are mechanical devices to measure tissue deficits within the field in both the transverse and the longitudinal body cross-sections. Examples of these systems include Ellis type filters [**43, 44**], rod boxes [**42**] and pantographic devices [**45**]. Recent devices include Moiré camera, 3-D magnetic digitizers, CT based compensator programs and electronic compensation using multileaf collimators [**10**]. Generally, the use of compensating filters instead of bolus is more laborious and time consuming. Besides this, the resulting dose distribution is not easily calculated on most treatment planning systems without measurement of the beam profile under the compensator and therefore additional beam data entry into the TPS.

2.8.6 Wedge filter

A wedge is the most commonly used beam-modifying device. It is a wedge-shaped absorber and causes a gradual decrease in the intensity across the beam. This leads to a tilt in the isodose curves from their perpendicular positions as shown in Fig. 2.9(b). They are generally made from lead or one of its low melting point alloys and are placed at least 15 cm from the skin so that electrons ejected from them do not contaminate the photon beam and eliminate the dose buildup effect at the patient's skin surface. There are three types of wedge filters currently in use: physical (manual), motorized and dynamic. The use of wedges tends to decrease the skin doses relative to the open fields, although this effect is small (<20% relative difference for a 60^{o} wedge). In contrast, dynamic wedges have negligible effect on the skin dose relative to the open field [**6, 46, 29**]. The angle through which these isodose lines are tilted is known as "wedge isodose angle". It is defined as the angle through which an isodose curve at a given depth in water (usually 10 cm) is tilted at the central beam axis under the condition of normal incidence. A combination of such identical distributions at right angles to each other gives a region of homogeneous dose distribution as in Figure 2.9**(c)** below.

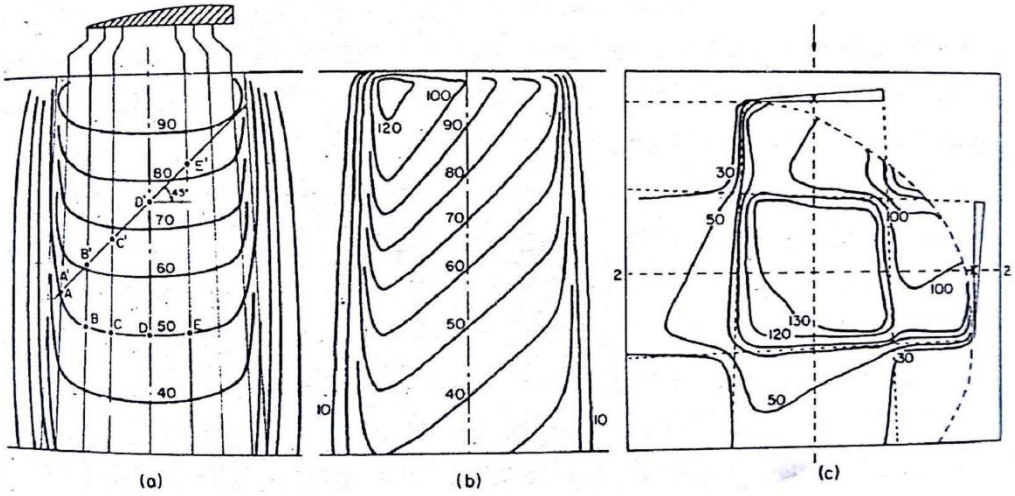

Figure 2. 9: (a) Design of a wedge filter to tilt the isodose lines through 45° for an 8 x 8 cm beam for a cobalt unit. (b) Isodose chart for the wedge of (a). (c) Dose distribution obtained by combining two wedged beams to produce a region of uniform dose distribution [**40**]

2.8.6.1 Physical wedges.

This is an angled piece of lead or steel that has either a straight or sigmoid surface shape. The first design is used to produce straighter isodose curves when it is placed in the path of the beam. However, manual intervention is needed to lift and place a physical wedge on the treatment unit's collimator assembly in a slot for the wedge on the ^{60}Co treatment machine or mounted on a transparent plastic tray which is then inserted into the beam at a specified distance from the source for a linear accelerator. This distance is such that the wedge and the tray are always at a distance of at least 15 cm from the skin surface. This way, the -sparing effect of the megavoltage beam is maintained.

2.8.6.2 A motorized wedge.

This is a similar beam modifying device to a physical wedge, but is integrated into the head of the treatment unit and is controlled remotely by machine.

2.8.6.3 Dynamic wedges.

These wedges are generated electronically by creating wedged beam profiles through the use of the independent collimator jaws to create wedge-shaped isodose distributions by moving one of the independent jaws while the other one remains stationary during irradiation. However, there is no clinical advantage of using dynamic wedges over the physical metallic wedges [**6**]. The clinical implementation of dynamic wedges during cancer treatment requires the measurements of central axis PDDs, central axis wedge transmission factors and transverse beam profiles of the dynamic wedge [**10, 11**, **47**].

2.8.7 Multileaf collimators (MLCs)

A multileaf collimator (MLC) for photon beams is a beam modifier that consists of a large number of leaves or collimating blocks that can be driven automatically and independent of each other in order to generate a field of any shape (Fig. 2.9). MLCs are therefore beam shaping devices that can replace almost all conventional mounted blocks, with the exception of shaping small fields or "island" blocking in which an area within the open portion of the fields needs to be blocked and excessively curved field shapes. Those providing smaller leaf widths are referred to as micro MLCs. They may be able to cover all or part of the entire field opening, and the leaf design may be incorporated into the TPS to model transmission and penumbra. They may also have varying degrees of dynamic motions that can be invoked while the beam is on in order to enhance dose delivery [**10, 41**].

2.8.7.1 Design of an MLC

A typical MLC system consists of 40 pairs of leaves or more e.g. models with 60 pairs of leaves covering fields of up to 40 × 40 cm^2. The leaves are made of tungsten alloy of density 17.0 to 18.5 g/cm^3 and have thicknesses along the beam direction that range from 6 cm to 7.5 cm, depending on the type of linear accelerator [**10**].

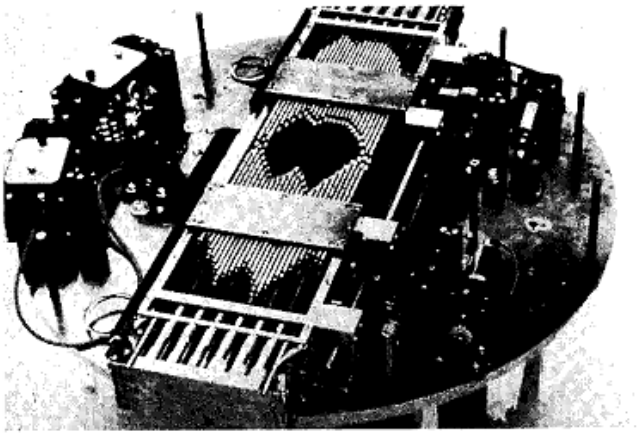

Figure 2. 10: Varian multileaf collimator attached to accelerator (Taken from Khan 2003, [**10]**)

The leaf thickness is usually sufficient enough to provide primary x-ray transmission through the leaves of less than 2% (compared with about 1% for jaws and 3.5% for cerrobend blocks) and an interleaf (between sides) transmission of less than 3%. The primary beam transmission is further minimized by combining jaws with the MLC in shielding areas outside the MLC field opening [**10, 41**].

Some MLC systems have double-focused leaves that form a cone of irregular cross-section diverging from the source position and move out on a spherical shell that is centered at the source. This provides a very sharp beam cut off at the edge of the field,

though this objective is achieved only to a limited extent for the high energy beams since the dose falloff at the edge is largely determined by scattered photons and electrons. Due to the difficulties in manufacturing double focused MLCs, some systems have been designed with rounded leaf edges to provide constant beam transmission through a leaf edge, regardless of its position in the field and with directions of travel perpendicular to the central ray.

An important consideration in the use of MLCs for stationary fields is the non-conformity between the planned field boundary which is continuous, and the jagged stepwise boundary created by the MLC. Optimization of MLC rotation and setting has been discussed by Brahme [**48**] where his analysis shows that the best orientation of the collimator is when the direction of motion of the leaves is parallel with the direction in which the target volume has the smallest cross-section.

2.8.7.2 Disadvantages of MLCs

(i) MLCs have a much larger physical penumbra than that produced by the collimator jaws or the cerrobend blocks. This is a drawback in case of treatment of small fields or when blocking is required close to critical structures.

(ii) Also, the jaggedness of the field edges makes it difficult to match adjacent fields, discrete size of the leaves require additional quality assurance with additional data requirement to characterize the output factors, central axis PDD and penumbrae.

2.8.7.3 Importance of MLCs in radiotherapy.

The following are the advantages of using MLCs in radiotherapy; (i) provision of automatic field shaping, (ii) the elimination of the need for storage facilities, (iii) the elimination of the need for technologies to lift heavy blocks, (iv) the ability to treat multiple fields without the need to re-enter the treatment room and (v) the modulation of beam intensity. Modern radiotherapy techniques such as 3-D conformal radiation therapy and IMRT are dependent on the dynamically controlled MLC. Other applications include dynamic wedges and electronic compensation [**10, 27, 41**].

CHAPTER THREE

MATERIALS AND METHODS

3.1 Introduction

The methodologies adopted to assess doses to the skin using calibrated GafChromic EBT2 films are presented in this chapter. Calibration of GafChromic EBT2 films for assessing skin dose with water equivalent (PMMA) phantom together with the dose measurements are outlined here in this chapter.

3.2 Materials

The materials used in this study includes; compensators (0.5 cm, 1.0 cm and 1.5 cm thickness), bolus (0.5 cm thickness), physical wedges (PW) (15°, 30°, 45° and 60°), motorized wedge (MW) (60°), barometer, digital thermometer, plastic water (PMMA) phantoms , ScanMaker 9800XL plus flat bedded scanner. Some specific materials are presented with details below.

3.2.1 GafChromic films

GafChromic EBT2 film with lot number; # 08221302 produced by the International Specialty Product with sheet size of 14" x 17" was used. The films were designed to measure doses up to at least 30 Gy when used with an RGB colour scanner. At doses above 10 Gy, the response in the red color channel approaches saturation, so in the case of single channel dosimetry, it is preferable to change to the green color channel for these

measurements. Figure 2.5 above shows the structure of GafChromic EBT2™ used in this work.

3.2.2 Ionization chamber

A cylindrical Farmer type ionization chamber manufactured by PTW Freiburg was used with the water equivalent (PMMA) phantoms to measure the transmission factors for the different beam modifiers used in this work. It has a sensitive air volume of 0.125 cm^3 that is open to the environment and therefore, its readings need to be corrected for factors like temperature, humidity and pressure that affect air density.

3.2.3 Electrometer

The electrometer used was PTW UNIDOS model with serial number T10005-50316. It was calibrated together with the ion chamber above. This was used to quantify charges that have been collected by the ionization chamber in nC/minute. The measured values were then corrected for temperature and pressure variations.

3.2.4 FilmQA™ Pro

FilmQA™ Pro is a sophisticated and quantitative analytical tool that is specifically designed to simplify and streamline IMRT QA process. The program allows one to scan or open images of exposed application films and calculate the optimized dose maps. This calculation is based on a scanner-dependent function generated from calibrated data that

are derived from the three color channels (red, green and blue). Figure 3.1 is a window in FilmQAPro 2015 that was used in this study.

When GafChromic™ films are used, the optimized dose maps include corrections for thickness artifacts by using the blue color channel to measure the absorbance of the yellow marker-dye in the films.

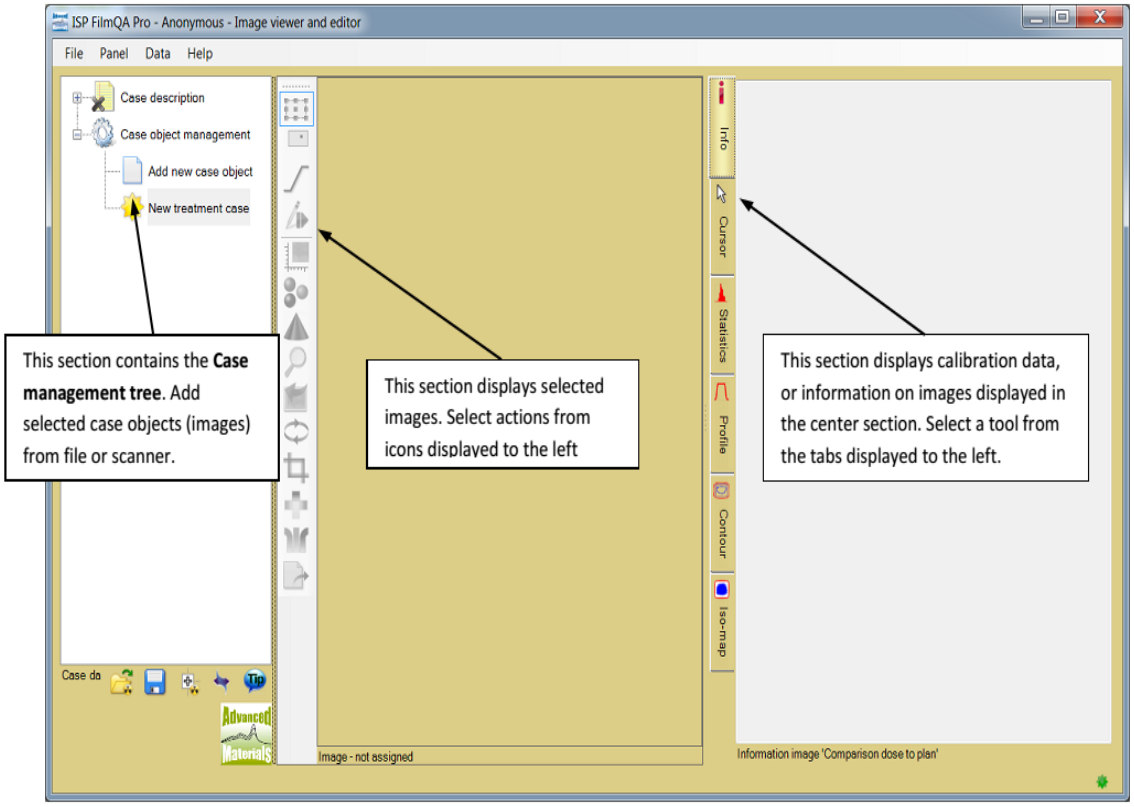

Figure 3. 1: A FilmQAPro2015 window showing the three main sections of; case management tree, image section and the analysis section.

3.3 Experimental method

3.3.1 Calibration of GafChromic EBT2 films.

Outlined precautionary measures for the handling of radiochromic films in TG-55 and [**35**] were used. The films with lot number #08221302 were kept within temperature range of 22^{o}C ± 2^{o}C during the experiment, storage and analysis. The film was only removed from the light tight envelope during irradiation and when it was being scanned using the flat bedded scanner.

Following the recommendations of the film manufacturer, the films from the same lot/batch were selected for calibration and were pre-cut into 6 × 8 cm^2 in order to have an area of at least 25 cm^2 as is specified in TG-55 and the manufacturer's calibration guidelines. These EBT2 films were then placed perpendicularly to the beam's central axis at a depth of 5 cm in a plastic water phantom of 30 × 30 × 20 cm^3. Two sets of films were considered.

Film set **A,** contained calibration films that were meant to measure doses for ^{60}Co. They were given known uniform radiation doses of 0.0 cGy, 20 cGy, 50cGy, 100 cGy, 150 cGy, 200 cGy, 500 cGy, 600 cGy, and 1000 cGy. Similarly, set **B** contained calibration films that were given uniform radiation doses in the range of 0-325 cGy, in increments of 25 cGy. The irradiations of both film sets were done using a uniform cobalt-60 radiation beam for a specified treatment time determined prior by the Prowess Panther TPS for a similar irradiation geometry and setup as for the actual irradiation of the calibration films.

These films were allowed to stay for 24 hours for post radiation development before being scanned using a ScanMaker 9800XL plus flat bedded scanner. Scanning of the films were done in landscape mode. Set **A** was read using FilmQAPro 2015 software and the values

plotted to obtain a calibration function that was used in converting the cobalt-60 exposed film responses to doses as indicated in Figure 4.1 below. Set **B,** on the other hand, was read using image J software and the responses were recorded as in Table B.1, appendix B. These values were plotted to give a calibration function as shown in Figure 4.2.

3.3.2 Measurements of transmission factors for the different beam modifiers used in this work.

A phantom measuring 30 × 30 × 20 cm^3 was setup on the cobalt-60 couch, perpendicularly along the beam central axis. A farmer type ion chamber of 0.125 cc measuring volume with a PTW UNIDOS electrometer were used to collect and measure charges collected respectively. The chamber was inserted in one of the phantoms (30 × 30 × 2 cm^3) having a hole at its sides with the center of the hole at a depth of 0.5 cm from the surface. Quality assurance (QA) was done on the unit prior to this measurements.

For an open field at SSD of 80 cm, field sizes of 8 x 8 cm^2, 10 × 10 cm^2, 15 ×15 cm^2, 18 × 18 cm^2, 20 × 20 cm^2 and 25 × 25 cm^2 were used to irradiate the ionization chamber for 1.0 minute. Charges were collected and measured using the electrometer. Three successive readings were taken for each field size and their average values determined. The initial and final temperatures and pressures were recorded using a thermometer and barometer respectively. The experiment was then repeated for all the other SSDs of 90 cm, 100 cm and 110 cm for the open beam. These measured values were then corrected for temperature and pressured as outlined in TG-51.

This same measurement was then repeated with the compensator (0.5 cm, 1.0 cm and 1.5 cm), tray of thickness 0.6 cm and the physical wedges (angles 15^0, 30^0, 45^0 and 60^0).

Transmission factors were then calculated for the different beam modifiers for the four SSDs above, and for the different field sizes used. This was done by dividing the corrected electrometer readings with and without the beam modifier in the path of the beam for each field size. These transmission factors were then used to determine the corresponding treatment times needed to deliver the same dose at d_{max} as that for an open beam for a particular square field. Plate 3.1 is a setup for measuring the transmission factor for the tray used in this work.

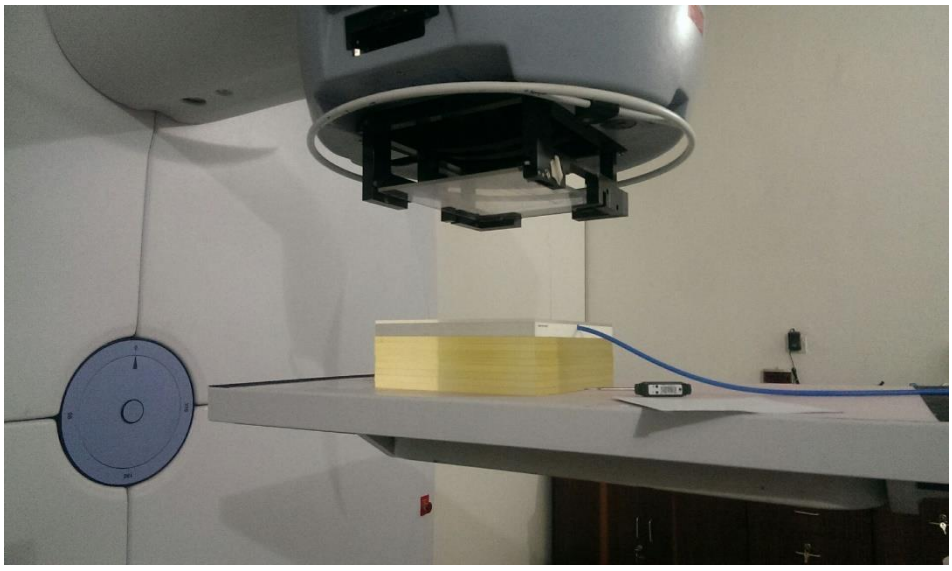

Plate 3. 1: Setup for measuring transmission factor for the tray.

3.3.3 Measurements of skin dose using GafChromic EBT2 film.

3.3.3.1 Setup and film irradiations.

Skin dose measurements were carried out using GafChromic EBT2™ films with lot number #08221302. They were cut into small pieces with dimensions of 2 × 3 cm^2 each and were labelled **A**, **B** and **C** for easy identification. Film set **A** was placed at the surface of the phantom, **B** at d_{max} and **C** at 10 cm depth. Film pieces of category **C** were then used in determining the PDD at 10 cm depth. This was then compared with the PPD at 10 cm depth for a cobalt beam. Two other film pieces measuring 30 × 30 cm^2 were cut and holes measuring 2.1 × 3.1 cm^2 was created at their centers for inserting the 2 × 3 cm^2 films. Plate 3.2 shows the phantom with film 30 × 30 cm^2 on top, having a film piece in a slot in it.

Plate 3. 2: A setup of showing the 2 × 3 cm^2 dose film in the slot in a bigger GafChromic film piece of dimension 30 x 30 cm^2 placed on top of the solid water phantom 30 × 30 × 20 cm^3.

Starting with SSD of 80 cm, set of films A, B and C were placed at the surface, d_{max}, and at a depth of 10 cm respectively. Field sizes of 8 x 8 cm^2, 10 × 10 cm^2, 15 × 15 cm^2, 18 × 18 cm^2, 20 × 20 cm^2 and 25 × 25 cm^2 were then used one at a time to expose the films for 60 seconds for the open beam. For each field size, the sets A, B and C were kept together in an envelope labelled with the field size and SSD. This same experimental procedures were repeated for all the other SSDs of 90 cm, 100 cm and 110 cm for the open beam.

The different beam modifiers (physical wedges, tray, and compensators) were then introduced in the beam at their correct positions, one at a time. The same procedures as described above were repeated for the different field sizes and SSDs as for the open beam. The sets of A, B and C were also kept in an envelope that has been labelled with the field size, SSD and the beam modifier used. The exposed films together with an unexposed one were then kept for 24 hours for post radiation exposure developments. During the irradiation, storage and scanning, the films were kept at a temperature of 22^oC ± 2^oC by using the air conditioner to ensure stable temperature range.

The above experimental setup and procedures were also used to determine skin doses from the linear accelerator (15 MV photons) at SGMC for motorized wedge 60°, open beams and for bolus (0.5 cm). This treatment machine has capability of using two photon energies of 6 MV and 15 MV and three electron energies of 6 MeV, 10 MeV and 15 MeV. The 15 MV photons was chosen for this work for the fact that it is the energy commonly used for treatment especially deep seated tumours. Field sizes used for these measurements were 5 × 5 cm^2, 10 × 10 cm^2, 15 × 15 cm^2, 20 × 20 cm^2 and 25 × 25 cm^2.

3.3.3.2 Scanning of irradiated dose films.

After 24 hours, the exposed films were removed and scanned using a 48-bit scanner; ScanMaker 9800XL plus. The scanner and the lid were cleaned of any dirt and the films were handled using surgical gloves to minimize fingerprints that may add errors to the readings. During the scanning process, the films were placed and scanned in a landscape mode just like the calibration films. This was done for the reason that the film response depends on whether it is scanned in portrait or landscape mode.

3.3.3.3 Reading of the exposed films from ^{60}Co.

The exposed films from the ^{60}Co beam were read using the FilmQAPro2015 software. Figure 3.4 below shows scanned film image set in the image section of FilmQAPro2015 software for dose reading, while the case management section shows the scanned films together with their dose maps.

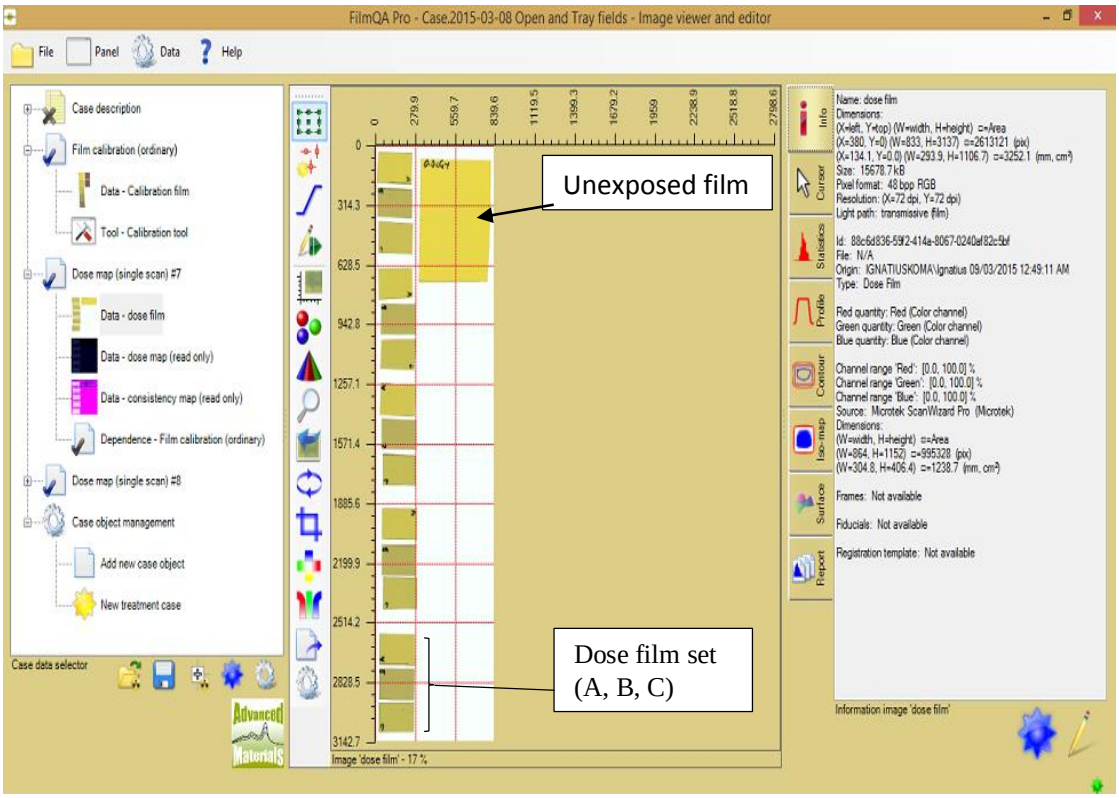

Figure 3. 2: A set of scanned film images for a tray at 110 cm SSD, field sizes 8 × 8 cm^2 to 25 × 25 cm^2.

A region is then selected in the middle of one film piece and duplicated in all the other films pieces for the other field sizes for that particular beam modifier. Using the calibration function in figure 4.1 below, the film's responses were then converted to doses. Figure 3.5 below, shows the analysis windows containing dose map in the middle and the analysis on the right.

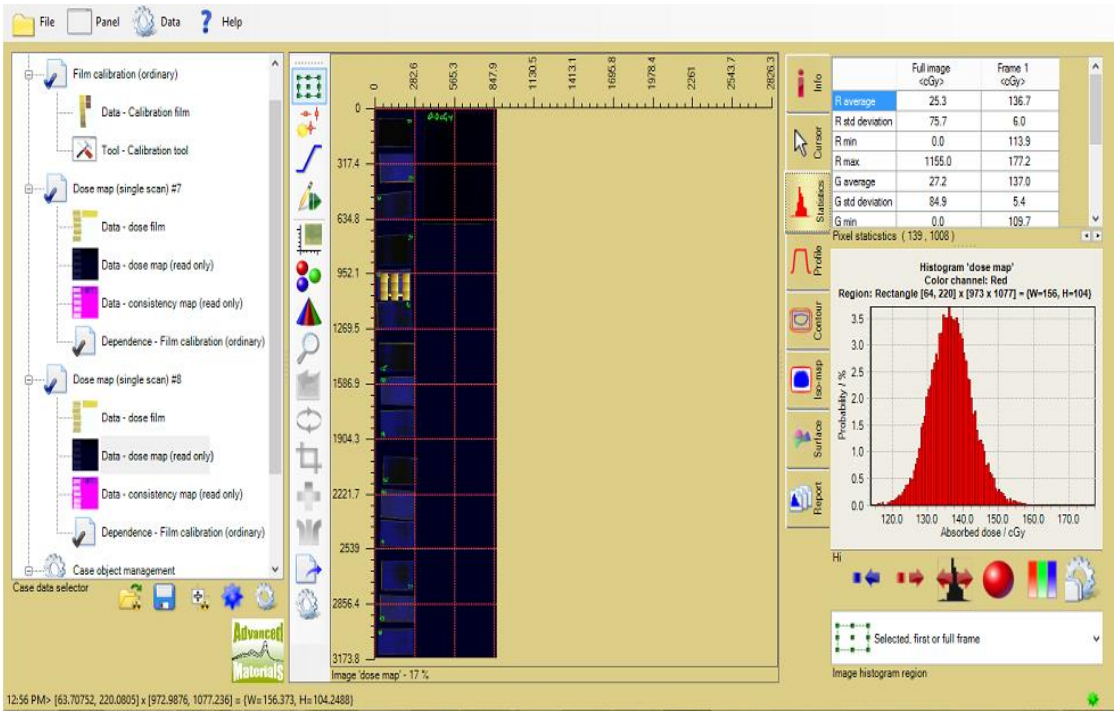

Figure 3. 3 shows a selected dose map in the image section and the corresponding average dose in the analysis section on the right.

This procedure was then repeated for all the other exposed films for the different beam modifiers, open fields and an unexposed film. The dose reading of the unexposed film was then subtracted from those of the exposed films. These dose readings were then recorded in an excel worksheet. The percentage skin doses were calculated by dividing the readings of film A (surface dose) by the readings of film B (d_{max} dose) and multiplying the results by 100. Similarly, the PDDs at 10 cm depth were obtained by diving the readings of films C by those of B and normalizing the result to 100%.

3.3.3.4 Reading of the dose films from the 15 MV photons.

Following the same procedures employed for the cobalt-60 dose films above, the 15 MV photon dose films were scanned using the 48-bit scanner; ScanMaker 9800XL plus. These

scanned films were then read using Image J film software. The response values (grey values) were then recorded and using the calibration Equation 4.1, these readings were converted into doses. Table B.2 in appendix B shows the measured skin doses from the 15 MV photons. The percentage skin doses for the 15 MV photons were determined for the bolus (0.5 cm), open fields and the MW (60°) for SSDs of 80 cm and 100 cm as was done for the cobalt-60 irradiated films. Table D.2, in appendix D shows the calculated percentage skin doses for the open beam, bolus and MW for the two SSDs considered in this work.

CHAPTER FOUR

RESULTS AND DISCUSSIONS

4.1 Introduction

This chapter discusses the results of the skin doses measured during the period of October 2014 to May 2015 at Radiotherapy Center of Korle-Bu Teaching Hospital and Sweden Ghana Medical Centre, using GafChromic EBT2 films. These doses were measured along the beam central axis and were expressed as a percentage of the dose at d_{max}. A discussion of the measured doses and the calculated percentage skin doses is presented in this chapter.

4.2 Calibration curve

Table 4.1 below gives measured optical density (OD) as a function of absorbed dose (cGy) for the calibration film set **A**.

Table 4. 1: Optical density (OD) as a function of absorbed dose for calibration film set A.

Absorbed dose (cGy)	Red (OD)	Green (OD)
1000	0.285	0.468
600	0.246	0.348
500	0.228	0.312
200	0.160	0.189
150	0.139	0.163
100	0.115	0.137
50	0.082	0.110
20	0.053	0.084
0	0.033	0.068

Figure 4.1 below is a plot of the optical densities against the absorbed doses for the calibration film set **A.**

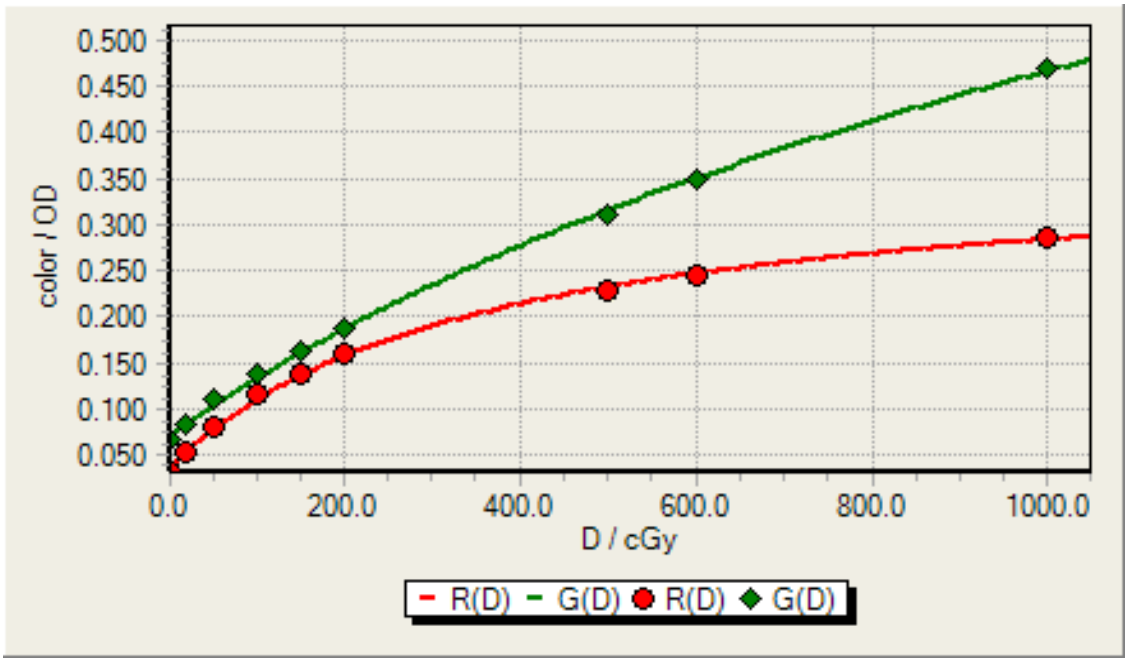

Figure 4. 1: Calibration functions for the two colour channels of red and green used in this work.

From the graph above, -R(D) is the graph of optical density against absorbed dose (D) for the red colour channel and -G(D) is the corresponding graph for green colour channel.

For film set **B**, three readings of exposed films were recorded and their average values calculated as is presented in Table B.1. The corresponding calibration function is presented in Figure 4.2 below.

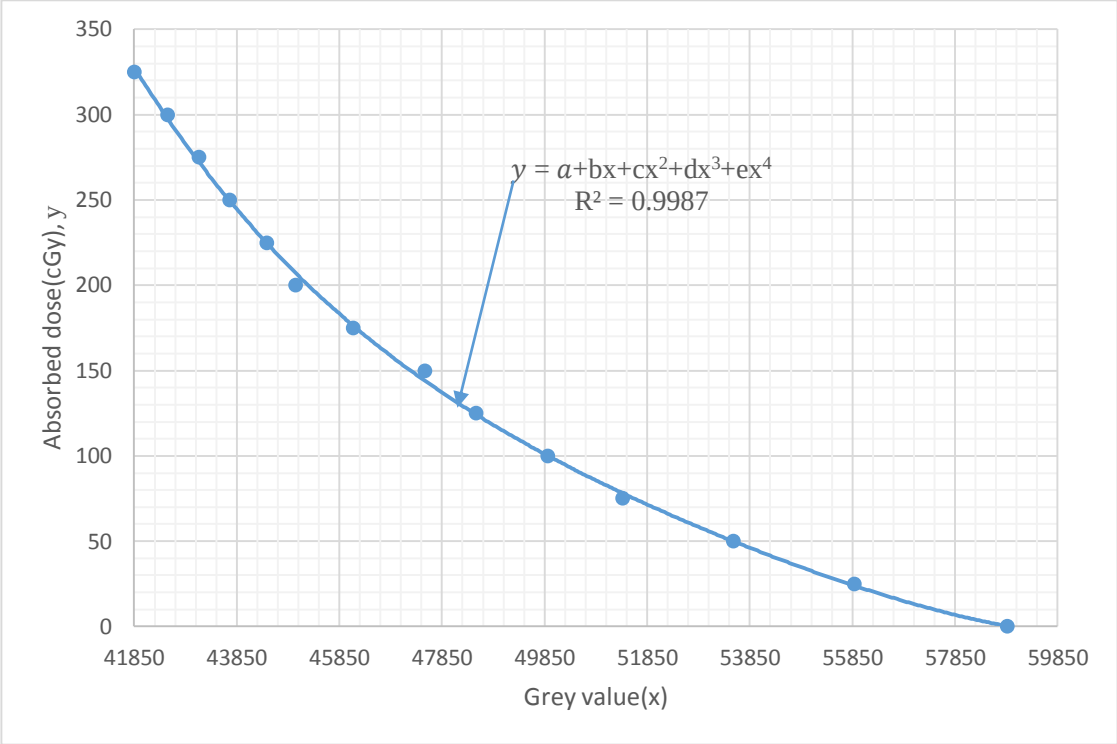

Figure 4. 2: A calibration graph for films set B read using image J software.

The corresponding calibration equation obtained from the above graph for the conversion of the film responses to dose is given as:

$$y = a + bx + cx^2 + dx^3 + ex^4 \quad \text{.....} \quad 4.1$$

where a = 7197.7203, b = -0.27757, c = 1.64E-06, d = 4.67E-11, e = -5.04E-16 and the regression $R^2 = 0.9987$.

The associated mean error in the calibration function was about 3% as is indicated in Table E.1 of appendix E.

4.3 Measured skin doses.

Tables A (1- 4) in appendix A, give the values of doses measured from the ^{60}Co treatment unit at KBTH. Measurements were taken at the surface (d = 0 cm, taken as skin dose) and for a depth of maximum dose, d_{max} (d = 0.5 cm) in PMMA slab phantom for the four SSDs. Table B.2 in appendix B on the other hand gives corresponding dose values measured from the Synergy 11 linear accelerator (15 MV photon) at SGMC. Errors in the measured values were minimal for most measured values. These errors were mainly from temperature and humidity variations and finger prints during cutting and scanning which amounts to a mean value of 3% as indicated in Table E.2 of appendix E.

For each field size, the ratio of skin dose (dose at d = 0 cm) to maximum depth dose (dose at d = 0.5 cm for ^{60}Co and d = 2.5 cm for 15 MV) was calculated. These values are shown in appendix C, Tables C.1-C.4 and appendix D, Table D.1. The calculated percentage skin doses for the open field ranges from 23.5% - 61.5% of the d_{max} dose for cobalt-60. These values fall within the 20% - 85% of the d_{max} dose that is given in skin dose during radiotherapy [**6**]. For the 15 MV photons, measured skin dose (as percent of d_{max} dose) ranges from 8.3% - 34.6% as compared to the findings of Stephen et al, 2012 [**6**], where the values they got ranged from 5.8% to 34.56%. A detailed analysis of these results gives the following observations.

4.3.1 Effect of field size on skin dose.

As in Tables A.1-A.4 of appendix A and table B.2 of appendix B, measured skin doses increased as field sizes were increased. This increase in skin dose with field size occurs for both the open beam and the ones with the beam modifiers. This is mainly as a result

of the increase in electron scattering from the collimators, air and any other material in the path of the beam like the beam modifiers. This is in agreement with other results in literature [**6, 10**], all of which reported an increase in skin dose with increasing field size.

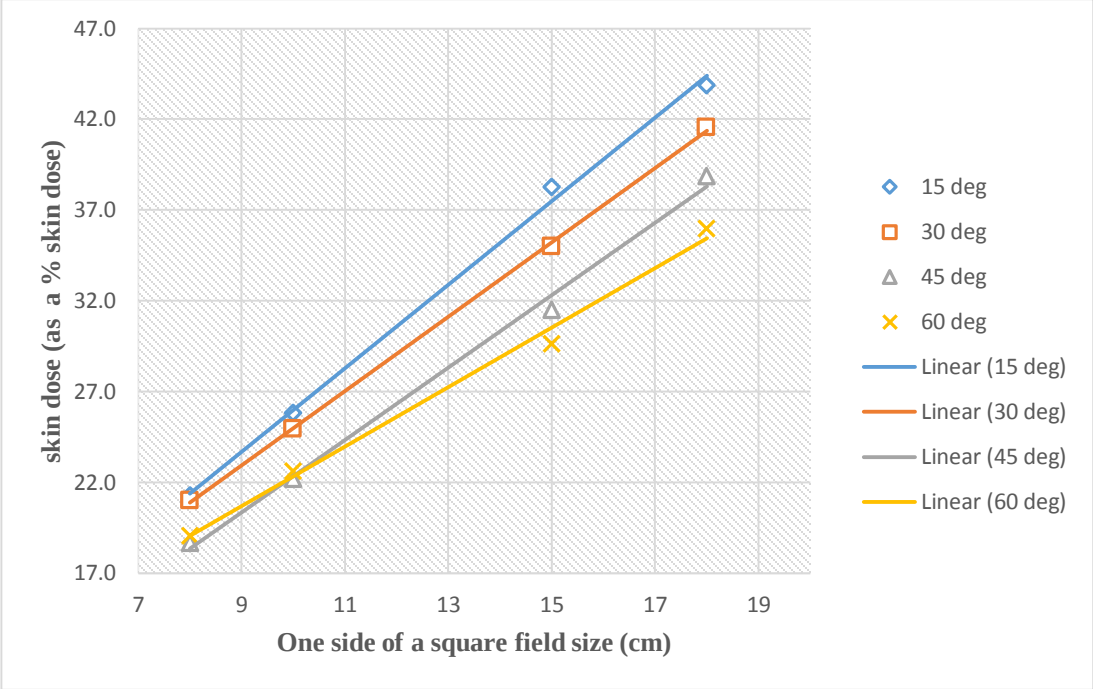

Figure 4. 3: Comparison of the skin dose for the four physical wedge angles at 80 cm SSD.

4.3.2 Effect of physical wedge on skin dose

For ^{60}Co, the use of PW reduced the skin doses as compared with the open beam, with the maximum reduction occurring at small field sizes and lower SSDs (80 cm and 90 cm) as compared with the larger SSDs (100 cm and 110 cm). Figure 4.3 shows the effect of the wedge angle on the skin dose for 80 cm SSD. It was observed that, as the wedge angle was increased, the skin sparing effect was also increased, but not for the larger angle (60°) especially at larger SSDs where it was reduced. This increase in skin sparing as the wedge angle increases is as a result of more scattered electrons being eliminated upstream the

PW than the ones generated downstream. This is in agreement with result presented by Nadir et al, 2002 [**49**]. For the larger SSDs (100 cm and 110 cm) and larger fields, the 45° and 60° PW produced higher skin dose as compared to all the other wedge angles, e.g. measured skin doses for 10 × 10 cm^2 were 25.1%, 23.3%, 21.3% and 26.8% for 15°, 30°, 45° and 60° respectively at 110 cm SSD. This could possibly be due to more scattered photons and electron contributions from the larger fields.

4.3.3 Effect of compensator thickness on skin dose.

For the compensator, it was observed that as the thickness of the compensator was increased, the percentage skin dose from the ^{60}Co reduced. This reduction in percentage skin dose with compensator thickness is as a result of the removal of more scattered electrons reaching the compensator compared to the ones incident on it. The overall result was that the percentage skin dose for the compensator fields was lower than the ones for the open field as it is reflected in Figure 4.4 below for SSD of 100 cm.

Generally, skin sparing effect of the compensator as compared to the open beam was better with higher effect seen at smaller field sizes. This effect then reduces as the field size was increased. This was reflected in the differences between the skin doses (as % of d_{max} dose) for the open beam and 1.5 cm thick compensator beam at 90 cm SSD where the values were 11.6%, 10.0%, 9.4%, 9.0%, and 4.9% for field sizes of 8 × 8 cm^2, 10 × 10 cm^2, 15 × 15 cm^2, 20 × 20 cm^2 and 25 × 25 cm^2 respectively. Lower skin doses were obtained at higher compensator thickness. At 80 cm SSD, skin dose for the 0.5 cm thickness compensator is almost the same as that of the open field at smaller fields but

increased quickly and became higher than those from the open beam. This is likely due to increased photon and electron scattering with field size.

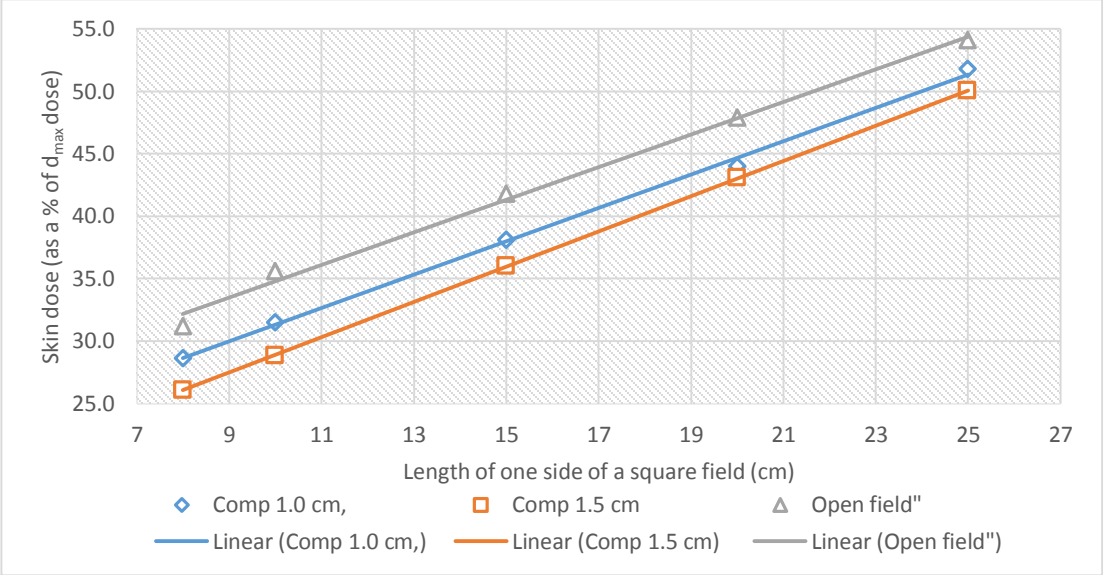

Figure 4. 4: A comparison of skin doses (as a % of d_{max} dose) for the compensator fields and open fields for SSD of 110 cm. Data was obtained from Equinox 100 ^{60}Co treatment machine at Korle Bu National Centre for Radiotherapy and Nuclear Medicine.

4.3.4 Effect of SSD on skin dose.

These research results also show that, as the SSD increases, the dose that the skin receives during treatment reduces. This reduction in skin dose with increasing SSD is attributed to the reduction in scattered electrons reaching the skin as compared to the smaller SSDs in which scattered electrons from the collimator and treatment heat reach the skin. This in turn leads to a reduction in deposition of dose at the skin surface. For 15 MV photons, measured skin doses (as % of d_{max} dose) for open beam 10 × 10 cm^2 were 14.0% and 12.0% for the SSDs of 80 cm and 100 cm respectively. This result agrees with the finding

of Yadav et al, 2010 [**50**]. They found skin doses for 15 MV, 10 × 10 cm^2 open beam to be 13.32% and 11.71% for SSDs of 80 cm and 100cm. The effect of SSDs on skin dose for cobalt-60 is shown in Table 4.2 (a) and (b), for the open beam and compensator (1.5 cm thickness) beams respectively, while Figure 4.5 is for the 15 MV photons, open beam. However, for the extended SSDs of 110 cm, there is an increase in skin dose for the cobalt-60 irradiations as compared with those for 100 cm SSD. This effect however, is gradually reduced as field size is increased. This increase in skin dose for the extended SSD could be as a result of increased scattering of photons and electrons with field size. Furthermore, for the extended SSD of 110 cm, the treatment couch is closer to the floor and more back scattered electrons and photons will be reaching the skin surface and depositing dose there.

Table 4. 2: Effect of SSD on the percentage skin dose for open beam and 1.5 cm thickness compensator beam from the Equinox 100 ^{60}Co treatment unit at Korle-Bu National Centre for Radiotherapy and Nuclear Medicine.

% Skin doses for open beam				
	SSD (cm)			
FS	**80**	**90**	**100**	**110**
8	33.7	33.3	23.5	31.2
10	36.9	36.5	26.5	35.6
15	45.1	44.0	33.9	41.8
20	54.0	52.0	41.5	47.9
25	61.8	60.0	54.0	54.1

(a)

% skin doses for 1.5 cm thick compensator				
	SSD (cm)			
FS	**80**	**90**	**100**	**110**
8	23.6	21.7	18.8	26.1
10	25.6	26.5	24.2	28.8
15	36.3	34.6	33.5	36.0
20	44.1	43.0	42.0	43.0
25	58.9	55.1	50.2	50.0

(b)

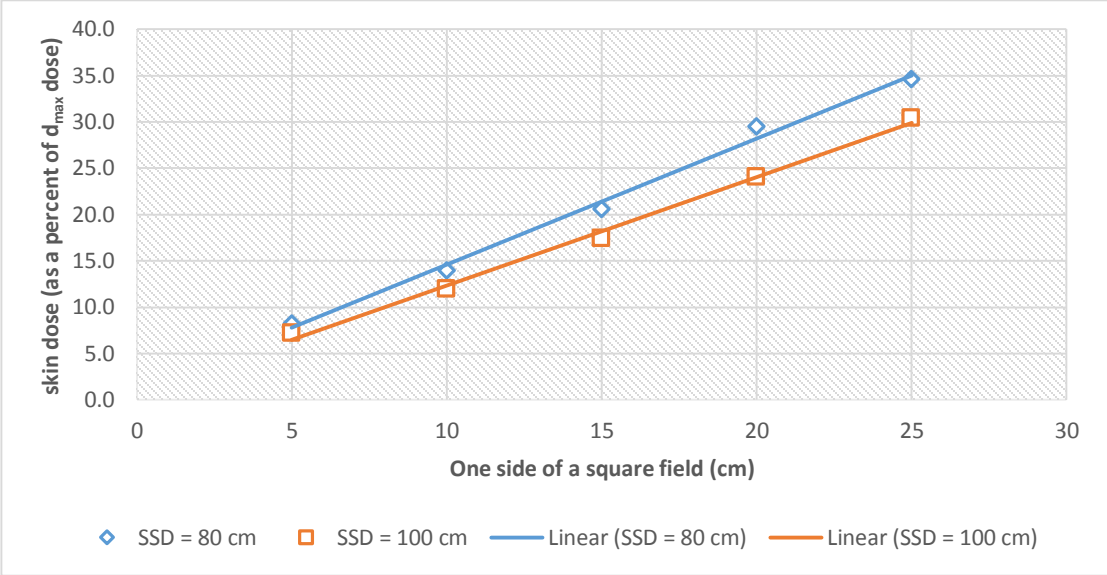

Figure 4. 5: Effect of SSD on skin dose (as a % of d_{max} dose) for 15 MV photon, open beam.

4.3.5 Effect of beam energy on skin dose.

Analysis of the results from the cobalt-60 and 15 MV shows that, the 15 MV photons produced a lower skin dose as compared with the cobalt-60. For cobalt-60 open beam, skin dose (as a % of d_{max} dose) for SSD of 100 cm were; 26.5%, 33.9%, 41.5% and 54.0% for field sizes of 10 × 10 cm^2, 15 × 15 cm^2, 20 × 20 cm^2 and 25 × 25 cm^2 respectively. For the same SSD and field sizes as for the cobalt-60, the values were; 12.0%, 17.4%, 24.0% and 30.4% for the 15 MV open beam. This result clearly shows the advantage of using high energy photons for cancer treatment as compared to cobalt-60. There is more skin sparing from the 15 MV photon as compared to cobalt. This result is in agreement with result in Stephen et al, 2011 [**6**]. Their measured skin doses for cobalt-60 ranged from 20% - 85% of d_{max} dose for field sizes ranging from 5 × 5 cm^2 to 40 × 40 cm^2 as compared to high energy photons (15-18 MV) where the values range between 8% - 45%

of the D_{max} dose for the same conditions as for the ^{60}Co. Figure 4.6 below shows skin doses for cobalt-60 versus 15 MV photons for 80 cm SSD.

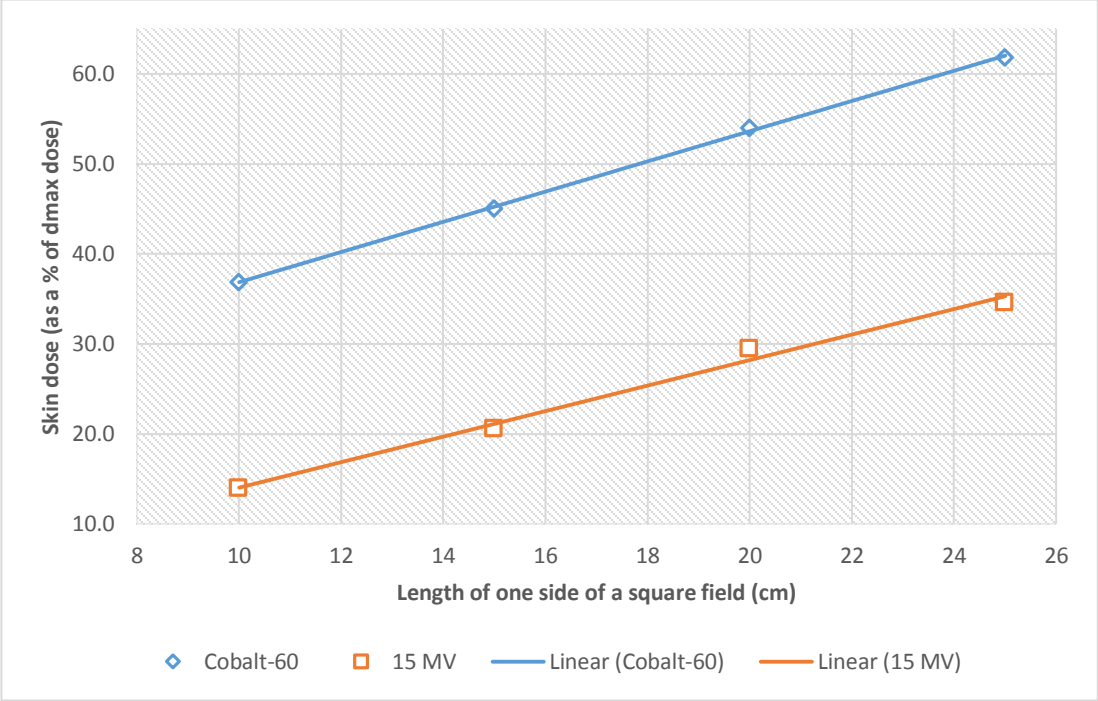

Figure 4. 6: A comparison between skin dose for cobalt-60 and the 15 MV for 80 cm SSD open beam.

4.3.6 Effect of motorized wedge 60° (MW) on skin dose.

The use of motorized wedge in treatment of cancer with the 15 MV x-rays generally has negligible effect on skin dose for the 80 cm SSD as compared with the open beam. For this SSD, measured skin doses for the MW beam were 8.8%, 12.5%, 19.3%, 27.5% and 36.2% for field sizes of 5 × 5 cm^2, 10 × 10, 15 × 15, 20 × 20 and 25 × 25 cm^2 respectively. This result agrees with that published by Yadav et al, 2010 [**50**]. Their measured skin doses were; 3.98%, 11.32%, 19.33, 28.13% and 35.03% for the same SSD and field sizes as above. Figure 4.7 is a graphical presentation of the effect of the MW on skin dose for

100 cm SSD. This however shows that, skin dose for the 60° MW increases rapidly as field size is increased compared with the open beam. This could be as a result of more scatter electrons being generated by the 60° MW than those being eliminated upstream.

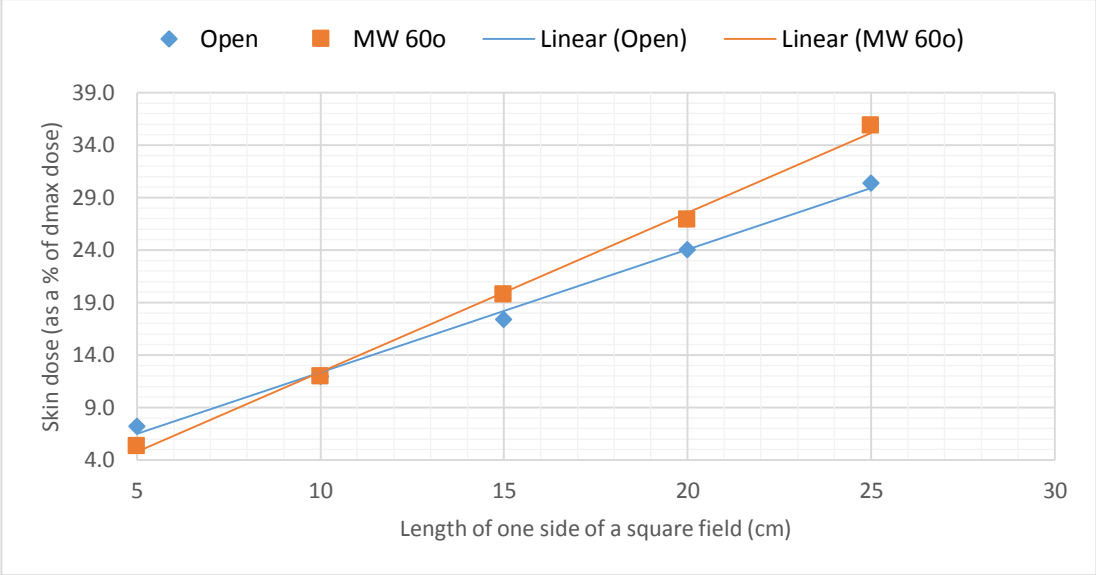

Figure 4. 7: Comparison skin dose for motorized wedge and open beam for 100 cm SSD.

4.3.7 Effect of bolus on skin dose.

Just like the other beam modifiers, measured skin doses for the bolus increased with increasing field sizes, but their values are much higher than those of the open beam. The use of bolus generally shifts the d_{max} upwards towards the skin surface, hence the high skin dose compared with the open beam. Measured skin dose for 10 x 10 cm^2, and 20 x 20 cm^2 fields were 57.4% and 68.8% for bolus at 100 cm SSD. The corresponding values for open beam were 12.0% and 24.0%. This shows that the skin dose due to the use of 0.5 cm thick bolus is about 45% higher than for open beam.

CHAPTER FIVE

CONCLUSIONS AND RECOMMENDATIONS

5.1 Conclusions

Dosimetric effects of beam modifiers use in external beam radiotherapy on skin or surface doses were studied for a solid water phantom for beam energies of cobalt - 60 and 15 MV. The skin doses are measured with Gafchromic films (EBT 2) for various field sizes and source to surface distances. The measured skin doses are compared to depth doses measured within the phantom for the same collimator setting and treatment time or monitor unit. Sensitometric curves of the film batch used in the study are generated with a film dosimetry software. Doses received by irradiated films are read by the film dosimetry software. Skin dose is found to increase with increasing field size for both beams with and without beam modifiers for all the beam energies used. Also skin dose decreases with increasing SSD (from 80 cm to 100 cm) for all the beam energies. However, for SSDs greater than 100 cm, skin dose tends to increase with increasing SSD for the cobalt-60 beam. The increase in the skin dose for the extended SSD may be attributed to the effects of beam divergence and scattered radiation reaching the surface of the phantom from the floor of the treatment room as the phantom is much closer to the floor. The 15 MV photon beam provides a better skin sparing compare to cobalt-60 beam for all field sizes and SSDs. These results show that the doses that the skin receives during external beam radiotherapy can be very high for larger field sizes, especially for open beams and beams with bolus at shorter SSDs. The highest skin dose compare to that of an open beam is obtained for a bolus (about 45 % higher than that for the open field) for the 15 MV photon beam. The highest reduction in skin dose for ^{60}Co on the other hand, is

obtained from the use of a physical wedge (45°) and is less than that for the open beam by 15.6%.

It can generally be concluded that most beam modifiers use for external beam radiotherapy at the two oncology institutions where the study was conducted lead to enhancement of the skin spare effect of the megavoltage beam, which is at its peak for beams with physical wedges. On the other hand, the use of a bolus and a tray during external beam radiotherapy increases skin dose. The maximum percentage skin dose deviation is measured was about 3.5 % as compared with that measured by Buston .M.J. [**27**] where the value was 4%. These discrepancies may be due to disparity in collimator design.

5.2 Recommendations

The use of extremely large field sizes for treatment should be discouraged as it compromises on the skin sparing effect of the megavoltage beam. In place of the large field size, two smaller adjacent field sizes can be used such that they are matched with an appropriate radiation field matching technique.

When beam modifier are used, they should be placed at distances ranging from 15 to 20 cm from the skin to reduce skin dose.

5.3 Further study

Since there are inherent error or uncertainties associated with film dosimetry the skin dose measurements need to be repeated with parallel plate ionization chamber. The dose readings obtained with the parallel plate ionization chamber should be compared with those measured with the film. This would improve on the findings of the study.

REFERENCES

1. Yadav, G., Yadav, R, Kumar, A. Skin dose estimation for various beam modifiers and source-to-surface distances for 6 MV photons. J Med Phys 2009; 34:87-92. doi:10.4103/0971-6203.51935. http://www.jmp.org.in/text.asp?2009/34/2/87/5135.
2. Nilsson B, Brahme A. (1986). Electron contamination from photon beam collimators. Radiother Oncol 1986; 5:235- 44. [PUBMED]
3. ICRU report 50. Prescribing, Recording, and Reporting Photon Beam Therapy. Med Phys. 21, 833 (1994); http://dx.doi.org/10.1118/1.597396
4. Flakus F.N. Detecting and measuring ionizing radiation- A short history. IAEA Bulletin, Vol 23; No 4. Pp 33.
5. American Association of Physics in Medicine (report 85). Tissue inhomogeneity correction for megavoltage photon beams. Medical Physics publishing, 2004.
6. Stephen F. Kry, Susan A. Smith, Rita Weathers, and Marilyn Stovall. Skin dose during radiotherapy: A summary and general estimation technique. Journal of Applied Clinical Medical physics, 2012; Vol 13, number 3.
7. International Commission on Radiological Protection. Recommendations of the International Commission on Radiological Protection. ICRP Publication 26. Oxford, UK: Pergamon Press; 1977
8. International Commission on Radiation Units and Measurement. Determination of dose equivalents resulting from external radiation sources. ICRU Report 39. Washington DC: ICRU 1985.
9. Lamb A. & Blake S. Investigation and modelling of the surface dose from linear accelerator produced 6 and 10 MV photon beams. Phys Med Biol 1998; 43(5):1133–46.
10. Khan F.M. The Physics of Radiation Therapy, third edition. Lippincott Williams & Wilkins 2003; pp 205-285.
11. Podgorsak E.B. Technical Edition. Radiation Oncology Physics: A Handbook for Teachers and Students. International Atomic Energy Agency, Vienna, 2005.
12. Rao PX, Pillai K, Gregg EC. Effect of shadow trays on surface dose and buildup for megavoltage radiation. AJR; 1973; 117:168.
13. Marbach JR, Almond PR. Scattered photons as the cause of the observed d_{max} shift with field size in high-energy photon beams. Med Phys 1977; 4: 310. http://dx.doi.org/10.1118/1.594319
14. Biggs PJ, Ling CC. Electrons as the cause of the observed d_{max}, shift with field size in high energy photons beams. Med Phys 1979; 6: 291.
15. Gerbi BJ, Khan FM. Measurement of dose in the buildup region using fixed-separation plane-parallel ionization chambers. Med Phys 1990; 17: 17.
16. Stathakis S, Li JS, Paskalev K, Yang J, Wang L, Ma CM. Ultra-thin TDs for skin dose determination in high energy photon beams. Phys Med Biol 2006; 51(14):3549–67.
17. Butson M.J, Yu PKN, Metcalfe PE. Measurement of off-axis and peripheral skin dose using radiochromic film. Phys Med Biol; 1998: 43(9): 2647–50.
18. Johns HE, Rawlinson JA. Desirable characteristics of high-energy photons and electrons. In: Kramer S, Suntharalingam N, Zinniger GF, eds. High energy photons and electrons. New York: John Wiley & Sons 1976; 11.
19. Saylor WL, Quillin RM. (1971). Methods for the enhancement of skin sparing in cobalt-

60 teletherapy. AJR; 111:174.
20. Hine GJ. Secondary electron emission and effective atomic numbers. Nucleonics; 1952; 10:9.
21. Khan FM. Use of electron filter to reduce skin dose in cobalt teletherapy. AJR; 1971; 111:180.
22. Burkell C.C., Watson T.A., Johns H.E. Skin effects of cobalt 60 telecurie therapy. Br J Radiol; 1954; 27:171.
23. Gagnon WF, Peterson M D. Comparison of skin doses to large fields using tangential beams from cobalt-60 gamma rays and 4 MV x-rays. Radiology 1978; 127:785.
24. Jackson W. Surface effects of high-energy x-rays at oblique incidence. Br J Radiol 1971; 44:109.
25. Orton CG, Seibert JB. Depth dose in skin for obliquely incident ^{60}Co radiation. Br J Radiol 1972; 45:271.
26. Gerbi BJ, Meigooni AS, Khan FM. Dose buildup for obliquely incident photon beams. Med Phys 1987; 14:393.
27. Butson MJ, Cheung T,Yu.K. Variations in 6 MV x-rays radiotherapy buildup dose with treatment distance. Aust Phys Eng Sci Med 2003; 26:2
28. Klein EE and Purdy JA. Entrance and exit dose regions for a Clinac-2100C. Int J Radiat Oncol Biol Phys 1993; 27(2):429–35.
29. Rapley P. Surface dose measurement using TLD powder extrapolation. Med Dosim. 2006; 31(3):209-15. DOI: http://dx.doi.org/10.1016/j.meddos.2006.02.003
30. Martin J. Buston, Peter Kingdom. N. You, Peter E. Met calve. Extrapolated surface dose measurements with radiochromic film. Med. Phys 1999; 26 (3), 485-488.
31. Rawlinson J.A, Arlen D, Newcombe D. Design of parallel plate chambers for the buildup region dose measurements in mega voltage photon beams. Med Phys 1992; 19:641-8. [PUBMED].
32. IAEA technical report series 381. The Use of Plane Parallel Ionization Chambers in High Energy Electron and Photon Beams, Vienna 1997.
33. Azam Niroomand-Rad, Chair Charles Robert Blackwell, Bert M. Coursey. Radiochromic film dosimetry: Recommendations of AAPM Radiation Therapy Committee Task Group 55: Reprinted from medical Physics 1998; Vol. 25, Issue 11.
34. International specialty products. GafChromic® EBT2 self-developing film for radiotherapy dosimetry February 19, 2009 Revision 1. From database on World Wide Web.http://www.veritastk.co.jp/attached/2062/GAFCHROMICEBT2TechnicalBrief-Rev1.pdf.
35. User manual FilmQA™ Pro: Version: 3.0.4864.35322, July 30, 2013. Retrived 10/11/2014 from database on WorldWideWeb. (http://www.ashland.com/Ashland/Static/Documents/ASI/Advanced%20Materials/FilmQA_Pro_User_Guide_2013v2.pdf).
36. Martin J. Butson, Peter K. N. Yu, Peter E. Metcalfe. Extrapolated surface dose measurements with radiochromic film. Medical Physics, vol. 26, No. 3, 1999; 485-8
37. Stevens M.A., Turner J.R., Hugtenburg R.P. and Butler P.H. High resolution dosimetry using radiochromic film and a document scanner. Phys. Med. Biol. 41, 2357-2365 s1996d. doi:10.1088/0031-9155/41/11/008
38. Cameron J.K., Sunrharalinpn N, Kenney GN. Thermoluminescent dosimetry Madison: University of Wisconsin Press, 1968.

39. ATTIX, F.H., Introduction to Radiological Physics and Radiation Dosimetry, Wiley, New York 1986.
40. Harold Elford Johns, John Robert Cunningham. The Physics of radiology, 4TH Edition 1983.
41. Williams, J.R., Thwaites, D.I. (Eds.). Radiotherapy physics in practice, 2nd edition, Oxford University Press, Oxford New York 2000.
42. Khan F.M., Moore V.C, Burns DJ. The construction of compensators for cobalt teletherapy. Radiology 1970; 96:187.
43. Hall E.J., Oliver R. The use of standard isodose distributions with high energy radiation beams-the accuracy of a compensator technique in correcting for body contours. Br J Radiol 1961; 34:43.
44. Ellis F, Hall EJ, Oliver R. A compensator for variations in tissue thickness for high energy beam. Br J Radiol 1959; 32: 42.
45. Boge RJ, Edland RW, Matthes DC. Tissue compensators for megavoltage radiotherapy fabricated from hollowed Styrofoam filled with wax. Radiology 1974; 111:193.
46. Kim S, Liu CR, Zhu T.C, Palta JR. Photon beam skin dose analysis for different clinical setups. Med Phys 1998; 25:860-6. [PUBMED]
47. Cohen M, Burns J.E, Sears R. Physical aspects of cobalt-60 teletherapy using wedge filters. I. Physical investigation. Arta Radiol 1960; 53:401-413. Dosimetric considerations. Acta Radiol, 53:486.
48. Brahme A. Optimal setting of multileaf collimators in stationary beam radiation therapy. Strahlenther Onkol 1988; 164: 343.
49. Nadir Küçük, Ayhan KILIÇ, Gönül Kemikler, Lütfi Özkan, Kayihan Engin. Analysis of surface dose from high energy photon beams for different clinical setup parameters. Turk J Med Sci 2002; 32, 211-215.
50. Girigesh Yadav, R. S. Yadav R.S, & Alok Kumar. Effect of various physical parameters on surface and build-up dose for 15-MV X-rays. J Med Phys 2010; 35(4): 202–206.

APPENDIX A

Table A.1:

Table A. 1: Skin and d_{max} doses as a function of field size for an SSD of 80 cm. Doses are from Equinox 100 ^{60}Co treatment unit at Korle-Bu National Centre for Radiotherapy and Nuclear Medicine, March 2015.

DESCRIPTION	DEPTH (cm)	FIELD SIZE (cm^2)					
		8 x 8	10 x 10	15 x 15	18 x 18	20 x 20	25 x 25
Open field	**0.0**	78.04	88.91	114.50	-	146.41	169.81
	0.5	231.28	241.14	253.96	-	270.90	274.64
Tray (0.6 cm)	**0.0**	81.54	91.26	101.39	-	150.93	175.02
	0.5	230.41	236.30	256.59	-	267.55	275.93
Comp (0.5 cm)	**0.0**	72.20	85.17	112.26	-	139.29	168.41
	0.5	228.55	232.33	252.99	-	261.88	273.67
Comp (1.0 cm)	**0.0**	65.28	81.61	108.92	-	133.39	160.05
	0.5	222.93	223.68	239.04	-	246.90	264.16
Comp (1.5 cm)	**0.0**	50.99	58.42	87.48	-	109.66	157.72
	0.5	216.00	228.11	240.88	-	248.92	267.59
Bolus (0.5 cm)	**0.0**	237.52	239.62	256.00	-	267.19	282.85
	0.5	233.69	239.12	260.73	-	271.15	279.43
Physical Wedge (15^o)	**0.0**	50.47	63.10	103.23	122.00	-	-
	0.5	237.13	244.26	269.22	277.61	-	-
Physical Wedge (30^o)	**0.0**	45.90	59.33	85.83	105.60	-	-
	0.5	236.41	237.75	268.26	264.95	-	-
Physical Wedge (45^o)	**0.0**	44.13	55.85	81.85	104.92	-	-
	0.5	236.34	251.33	259.82	269.92	-	-
Physical Wedge (60^o)	**0.0**	43.66	52.36	75.92	97.18	-	-
	0.5	229.06	231.37	256.00	270.04	-	-

Table A. 2: Skin and d_{max} doses measured 90 cm SSD in PMMA slab phantom under Equinox 100 ^{60}Co treatment unit at KBTH.

DESCRIPTION	DEPTH (cm)	FIELD SIZE (cm^2)					
		8 x 8	10 x 10	15 x 15	18 x 18	20 x 20	25 x 25
Open field	**0.0**	63.19	69.75	92.67	-	111.49	130.96
	0.5	189.76	191.06	210.40	-	214.40	218.15
Tray (0.6 cm)	**0.0**	62.08	69.96	88.39	-	108.27	129.21
	0.5	185.59	188.50	198.91	-	212.03	211.72
Comp (0.5 cm)	**0.0**	43.79	62.76	78.38	-	104.50	129.61
	0.5	185.37	195.41	204.45	-	205.59	223.56
Comp (1.0 cm)	**0.0**	36.92	4647.00	66.84	-	95.81	120.49
	0.5	167.94	185.79	185.50	-	211.08	213.41
Comp (1.5 cm)	**0.0**	35.69	44.78	67.03	-	84.28	110.51
	0.5	164.41	168.67	193.50	-	196.19	200.48
Bolus (0.5 cm)	**0.0**	181.41	184.80	202.09	-	209.25	222.07
	0.5	184.37	188.50	197.84	-	210.61	215.31
Physical Wedge (15^0)	**0.0**	55.96	63.94	88.37	89.68	-	-
	0.5	179.59	187.64	208.81	200.11	-	-
Physical Wedge (30^0)	**0.0**	38.82	43.14	58.96	86.10	-	-
	0.5	184.97	186.74	201.01	208.11	-	-
Physical Wedge (45^0)	**0.0**	37.95	46.08	59.08	81.35	-	-
	0.5	190.01	187.82	207.02	214.19	-	-
Physical Wedge (60^0)	**0.0**	33.41	40.78	65.46	88.18	-	-
	0.5	188.23	186.17	202.83	206.58	-	-

Table A. 3: Measured skin and d_{max} doses for ^{60}Co at an SSD of 100 cm.

DESCRIPTION	DEPTH (cm)	FIELD SIZE (cm^2)					
		8 x 8	10 x 10	15 x 15	18 x 18	20 x 20	25 x 25
Open field	**0.0**	35.21	43.08	58.15	-	75.06	99.47
	0.5	150.12	162.28	171.38	-	180.84	184.12
Tray (0.6 cm)	**0.0**	34.37	41.50	59.36	-	74.95	99.60
	0.5	151.94	157.77	172.79	-	179.27	184.83
Comp (0.5 cm)	**0.0**	33.80	38.08	51.38	-	71.42	82.99
	0.5	154.33	162.58	170.01	-	172.21	183.54
Comp (1.0 cm)	**0.0**	43.51	51.43	66.84	-	82.84	98.60
	0.5	151.01	150.93	170.26	-	179.48	183.32
Comp (1.5 cm)	**0.0**	27.74	37.45	53.41	-	71.94	89.81
	0.5	147.44	154.81	159.36	-	171.36	178.82
Bolus (0.5 cm)	**0.0**	155.55	159.05	171.26	-	173.20	179.74
	0.5	155.05	156.24	171.81	-	180.00	176.74
Physical Wedge (15^0)	**0.0**	35.36	42.90	68.41	81.40	-	-
	0.5	160.78	162.90	175.46	185.00	-	-
Physical Wedge (30^0)	**0.0**	32.06	38.40	58.96	75.64	-	-
	0.5	159.27	166.65	177.61	175.69	-	-
Physical Wedge (45^0)	**0.0**	39.22	49.03	63.28	75.74	-	-
	0.5	157.12	162.13	170.90	177.41	-	-
Physical Wedge (60^0)	**0.0**	40.52	50.28	65.36	76.84	-	-
	0.5	157.01	164.62	173.30	175.87	-	-

Table A. 4: Measured skin and d_{max} doses for ^{60}Co at an SSD of 110 cm.

DESCRIPTION	DEPTH (cm)	SQUARE FIELD SIZES (cm2)					
		8 x 8	10 x 10	15 x 15	18 x 18	20 x 20	25 x 25
Open field	**0.0**	40.83	48.58	60.53	-	71.83	82.03
	0.5	130.86	136.53	144.83	-	150.02	151.73
Tray (0.6 cm)	**0.0**	42.34	46.94	54.44	-	71.94	84.20
	0.5	134.34	136.94	142.84	-	150.54	155.59
Comp (0.5 cm)	**0.0**	36.09	44.19	57.76	-	70.19	81.29
	0.5	128.57	138.03	147.74	-	152.23	149.35
Comp (1.0 cm)	**0.0**	35.72	41.98	51.01	-	63.18	76.64
	0.5	124.76	133.24	135.53	-	143.58	148.07
Comp (1.5 cm)	**0.0**	32.72	38.03	51.17	-	62.21	72.83
	0.5	125.46	132.02	142.08	-	144.55	145.59
Bolus (0.5 cm)	**0.0**	133.80	141.70	146.58	-	153.25	158.80
	0.5	134.70	140.51	148.32	-	155.79	162.09
Physical Wedge (15^0)	**0.0**	28.19	33.99	51.03	65.27	-	-
	0.5	131.17	135.32	149.10	153.32	-	-
Physical Wedge (30^0)	**0.0**	26.68	31.82	49.92	62.12	-	-
	0.5	132.61	136.40	146.81	151.55	-	-
Physical Wedge (45^0)	**0.0**	24.19	30.24	47.39	56.48	-	-
	0.5	133.55	142.14	151.93	151.40	-	-
Physical Wedge (60^0)	**0.0**	30.82	37.69	54.55	62.95	-	-
	0.5	137.92	140.68	146.55	146.75	-	-

APPENDIX B

Table B. 1: Measured calibration film responses as a function of exposure dose for calibration film set B.

DOSE (cGy)	Reading 1	Reading 2	Reading 3	Average reading	% Deviation
0	58740.1	58803.8	59057.4	**58867.11 ±137.1**	0.23
25	55731	55789.1	56134.8	**55884.96 ±178.2**	0.32
50	53324.6	53526.7	53751.7	**53534.34 ±174.4**	0.33
75	51233.8	51307.2	51595.6	**51378.83 ±156.2**	0.30
100	49823.7	49759.1	50153.5	**49912.12 ±172.7**	0.35
125	48397.8	48508.1	48646.4	**48517.44 ±101.7**	0.21
150	47428	47500.3	47626.2	**47518.20 ± 81.9**	0.17
175	46204.3	46191.1	45990.2	**46128.52 ± 98**	0.21
200	45086.7	44933.9	44963.2	**44994.60 ± 66.2**	0.15
225	44508.9	44637.1	44163.6	**44436.53 ±200**	0.45
250	43829.5	43854	43446.4	**43709.95 ±186.5**	0.43
275	43195.6	43248.9	42895.2	**43113.22 ±155.7**	0.36
300	42603.2	42645.2	42283.8	**42510.74 ±161.4**	0.38
325	41913.1	41908.9	41733.5	**41851.81 ±83.7**	0.20
			Percentage mean deviation		**0.29**

Table B. 2: Measured skin and dmax doses from Synergy 11 linear accelerator at SGMC for SSDs of 80 cm and 100 cm for 15MV.

DESCRIPTION	DEPTH (cm)	FIELD SIZE (cm^2)				
		5 x 5	10 x 10	15 x 15	20 x 20	25 x 25
MEASURED DOSE VALUES FOR 80 cm SSD						
Open field	**0**	11.59	21.19	34.18	46.35	54.53
	2.5	140.29	151.44	165.78	168.45	171.71
Bolus (0.5 cm)	**0**	106.73	138.76	164.8	193.45	203.77
	2.5	194.93	232.21	253.83	262.07	258.79
Motorized wedge (60°)	**0**	2.94	4.81	7.95	12.07	15.49
	2.5	33.33	38.41	41.14	43.98	42.76
MEASURED DOSE VALUES FOR 100 cm SSD						
Open field	**0**	8.77	16.42	25.54	36.51	41.73
	2.5	121.78	136.68	146.75	151.86	153.14
Bolus (0.5 cm)	**0**	67.21	77.62	97.57	105.45	166.23
	2.5	123.61	135.24	144.70	153.36	226.53
Motorized wedge (60°)	**0**	1.52	3.92	7.10	10.75	14.10
	2.5	28.31	31.17	35.89	39.93	39.32

APPENDIX C

Table C. 1: Percentage skin doses for an SSD of 80 cm from an Equinox 100 ^{60}Co treatment machine.

Calculated percentage skin doses ± 3%										
FS	**COMP 0.5 cm**	**COMP 1.0cm**	**COMP 1.5 cm**	**TRAY**	**OPEN**	**FS**	**Wedge 15 º**	**Wedge 30º**	**Wedge 45 º**	**Wedge 60 º**
8	35.4	29.3	23.6	35.4	33.7	**8**	21.3	19.4	18.7	19.1
10	38.6	36.5	25.6	38.6	36.9	**10**	25.8	25.0	22.2	22.6
15	39.5	45.6	36.3	39.5	45.1	**15**	38.3	32.0	31.5	29.7
20	56.4	54.0	44.1	56.4	54.0	**18**	43.9	41.5	38.9	36.0
25	63.4	60.8	58.9	63.4	61.8					

Table C. 2: Percentage skin doses for an SSD of 90 cm from an Equinox 100 ^{60}Co treatment machine.

Calculated percentage skin doses ± 3%										
FS	**Wedge 15^0**	**Wedge 30^0**	**Wedge 45^0**	**Wedge 60^0**	**FS**	**OPEN**	**TRAY 6mm**	**COMPENSATOR**		
								0.5 cm	**1.0 cm**	**1.5 cm**
8	31.2	21.0	20.0	17.7	8	33.3	33.4	23.6	22.0	21.7
10	34.1	23.1	24.5	21.9	10	36.5	37.1	32.1	25.0	26.5
15	39.9	29.3	32.0	32.3	15	44.0	44.4	38.3	36.0	34.6
18	44.8	41.4	38.0	42.7	20	52.0	51.1	50.8	45.4	43.0
					25	60.0	61.0	58.0	56.5	55.1

Table C.3: Percentage skin doses for an SSD of 100 cm from Equinox 100 ^{60}Co treatment machine.

Calculated percentage skin doses ± 3%										
FS	**Wedge 15^0**	**Wedge 30^0**	**Wedge 45^0**	**Wedge 60^0**	**FS**	**TRAY**	**COMP 0.5 cm**	**COMP 1.0 cm**	**COMP 1.5 cm**	**OPEN**
8	22.0	20.1	25.0	25.8	**8**	22.6	21.9	28.8	18.8	23.5
10	26.3	23.0	29.9	30.5	**10**	26.3	23.4	34.1	24.2	26.5
15	39.0	33.2	37.0	37.7	**15**	34.4	30.2	39.3	33.5	33.9
18	44.0	43.1	42.7	43.7	**20**	41.8	41.5	46.2	42.0	41.5
					25	53.9	45.2	53.8	50.2	54.0

Table C.4: Percentage skin doses for an SSD of 110 cm from Equinox ^{60}Co treatment machine.

Summary of measured percentage skin doses ± 3%										
FS	**Wedge 15^0**	**Wedge 30^0**	**Wedge 45^0**	**Wedge 60^0**	**FS**	**TRAY**	**COMP 0.5 cm**	**COMP 1.0 cm**	**COMP 1.5 cm**	**OPEN**
8	21.5	20.1	18.1	22.4	**8**	31.5	28.1	28.6	26.1	31.2
10	25.1	23.3	21.3	26.8	**10**	34.3	32.0	31.5	28.8	35.6
15	34.2	34.0	31.2	37.2	**15**	38.1	39.1	38.1	36.0	41.8
18	42.6	41.0	37.3	42.9	**20**	47.8	46.1	44.0	43.0	47.9
					25	54.1	54.4	51.8	50.0	54.1

APPENDIX D

Table D.1: Percentage skin doses for 15 MV at SSDs of 80 cm and 100 cm. Data was taken from the Synergy 11 linear accelerator treatment machine at Sweden Ghana Medical Centre.

Summary skin dose for 15 MV as a % of d_{max} doses (± 3%)							
	80 cm SSD				**100 cm SSD**		
FS	**BOLUS**	**OPEN**	**MW (60^0)**	**FS**	**BOLUS**	**OPEN**	**MW (60^0)**
5	53.8	8.3	8.8	**5**	54.4	7.2	5.4
10	59.8	14.0	12.5	**10**	57.4	12.0	12.0
15	64.9	20.6	19.3	**15**	67.4	17.4	19.8
20	73.8	29.5	27.5	**20**	68.8	24.0	26.9
25	78.7	34.6	36.2	**25**	75.9	30.4	35.9

APPENDIX E

Table E.1: Percentage error in calibration functions in Figures 4.1 & 4.2.

Grey value	Prescribed dose(cGy)	Measured Dose (cGy)	Difference (cGy)	% difference
55884.96	25	27.952	2.952	11.81
53534.34	50	50.808	0.808	1.62
51378.83	75	76.091	1.091	1.45
49912.12	100	97.553	-2.447	2.45
48517.44	125	122.277	-2.723	2.18
47518.20	150	143.068	-6.932	4.62
46128.52	175	176.882	1.882	1.08
44994.60	200	209.178	9.178	4.59
44436.53	225	226.758	1.758	0.78
43709.95	250	251.412	1.412	0.56
43113.22	275	273.215	-1.785	0.65
42510.74	300	296.709	-3.291	1.10
41851.81	325	324.169	-0.831	0.26
		Mean error		**2.55**

Table E.2. Errors in dose measurements using gafchromic EBT2 films

Grey value			Dose (cGy)	Measured dose (cGy)			Difference (cGy)			% error in measured value			Ave error
G1	G2	G3		M1	M2	M3	D1	D2	D3	E1	E2	E3	
55662.0	55832.6	56125.5	**25**	30.04	28.44	25.70	5.04	3.44	0.70	16.8	13.8	2.8	11.12
53108.4	53747.4	53753.2	**50**	55.35	48.60	48.54	5.35	-1.40	-1.46	9.7	-2.8	-2.9	1.32
51132.5	51382.6	51603.2	**75**	79.41	76.04	73.15	4.41	1.04	-1.85	5.6	1.4	-2.5	1.49
49854.6	49749.3	50153.8	**100**	98.48	100.21	93.72	-1.52	0.21	-6.28	-1.5	0.2	-6.3	2.54
48306.4	48653.3	48667.9	**125**	126.44	119.66	119.38	1.44	-5.34	-5.62	1.1	-4.3	-4.5	2.54
47339.9	47569.9	47629.9	**150**	147.07	141.92	140.61	-2.93	-8.08	-9.39	-2.0	-5.4	-6.3	4.55
46223.0	46181.9	45978.9	**175**	174.39	175.47	180.89	-0.61	0.47	5.89	-0.4	0.3	3.4	1.09
45227.4	44817.0	44966.1	**200**	202.18	214.65	210.05	2.18	14.65	10.05	1.1	7.3	5.0	4.48
44430.3	44747.4	44174.6	**225**	226.96	216.82	235.41	1.96	-8.18	10.41	0.9	-3.6	4.6	0.62
43842.2	43854.6	43438.8	**250**	246.77	246.34	261.14	-3.23	-3.66	11.14	-1.3	-1.5	4.5	0.56
43182.6	43306.8	42916.1	**275**	270.60	265.98	280.74	-4.40	-9.02	5.74	-1.6	-3.3	2.1	0.94
42561.3	42715.1	42271.7	**300**	294.68	288.57	306.45	-5.32	-11.43	6.45	-1.8	-3.8	2.2	1.15
41862.5	41934.4	41716.6	**325**	323.71	320.62	330.04	-1.29	-4.38	5.04	-0.4	-1.3	1.5	0.07

55729.0	55873.7	56143.0	**25**	29.41	28.06	25.54	4.41	3.06	0.54	15.0	12.2	2.2	9.79
53065.6	53760.3	53758.9	**50**	55.82	48.47	48.48	5.82	-1.53	-1.52	10.4	-3.1	-3.0	1.44
51150.8	51370.7	51575.8	**75**	79.16	76.20	73.51	4.16	1.20	-1.49	5.3	1.6	-2.0	1.62
49859.4	49716.2	50145.1	**100**	98.41	100.75	93.86	-1.59	0.75	-6.14	-1.6	0.7	-6.1	2.34
48298.3	48630.5	48663.3	**125**	126.60	120.09	119.47	1.60	-4.91	-5.53	1.3	-3.9	-4.4	2.36
47364.7	47600.1	47648.8	**150**	146.51	141.26	140.19	-3.49	-8.74	-9.81	-2.4	-5.8	-6.5	4.92
46229.4	46208.8	45985.2	**175**	174.22	174.76	180.72	-0.78	-0.24	5.72	-0.4	-0.1	3.3	0.90
45254.9	44813.3	44976.8	**200**	201.37	214.76	209.72	1.37	14.76	9.72	0.7	7.4	4.9	4.31
44428.2	44750.8	44190.2	**225**	227.03	216.72	234.89	2.03	-8.28	9.89	0.9	-3.7	4.4	0.54
43863.6	43849.5	43428.5	**250**	246.03	246.52	261.52	-3.97	-3.48	11.52	-1.6	-1.4	4.6	0.53
43177.1	43305.6	42917.6	**275**	270.81	266.03	280.68	-4.19	-8.97	5.68	-1.5	-3.3	2.1	0.92
42546.7	42701.2	42279.4	**300**	295.26	289.12	306.14	-4.74	-10.88	6.14	-1.6	-3.6	2.0	1.06
41898.0	41972.2	41730.1	**325**	322.18	319.01	329.45	-2.82	-5.99	4.45	-0.9	-1.8	1.4	0.45
55686.6	55832.5	56111.7	**25**	29.80	28.44	25.83	4.80	3.44	0.83	16.1	13.8	3.3	11.07
53041.5	53728.7	53729.6	**50**	56.08	48.79	48.78	6.08	-1.21	-1.22	10.8	-2.4	-2.4	2.00
51152.7	51360.3	51587.0	**75**	79.14	76.34	73.36	4.14	1.34	-1.64	5.2	1.8	-2.2	1.61
49841.6	49730.0	50130.1	**100**	98.69	100.52	94.09	-1.31	0.52	-5.91	-1.3	0.5	-5.9	2.24
48300.8	48607.8	48653.2	**125**	126.55	120.53	119.66	1.55	-4.47	-5.34	1.2	-3.6	-4.3	2.21
47339.5	47586.9	47626.6	**150**	147.08	141.55	140.68	-2.92	-8.45	-9.32	-2.0	-5.6	-6.2	4.61
46195.0	46170.3	45967.9	**175**	175.13	175.78	181.19	0.13	0.78	6.19	0.1	0.4	3.5	1.35
45244.7	44840.5	44963.2	**200**	201.67	213.92	210.14	1.67	13.92	10.14	0.8	7.0	5.1	4.28
44437.9	44713.2	44200.5	**225**	226.71	217.90	234.54	1.71	-7.10	9.54	0.8	-3.2	4.2	0.61
43824.2	43847.6	43486.2	**250**	247.40	246.58	259.42	-2.60	-3.42	9.42	-1.1	-1.4	3.8	0.45
43165.2	43286.9	42911.5	**275**	271.26	266.72	280.91	-3.74	-8.28	5.91	-1.4	-3.0	2.1	0.75
42558.9	42692.6	42268.1	**300**	294.77	289.46	306.60	-5.23	-10.54	6.60	-1.8	-3.5	2.2	1.03
41870.9	41941.0	41757.2	**325**	323.35	320.34	328.26	-1.65	-4.66	3.26	-0.5	-1.4	1.0	0.31
				AVERAGE ERROR IN MEASURED DOSE VALUES									**2.47**